Mechanical strain regulates contractile protein dynamics related to heart remodeling

BY

Erik R. Swanson
B.S., Rensselaer Polytechnic Institute, 2008

THESIS

Submitted as partial fulfillment of the requirements
for the degree of Master of Science in Physiology and Biophysics
in the Graduate College of the
University of Illinois at Chicago, 2012

Chicago, Illinois

Defense Committee:

R. John Solaro, Chair
Brenda Russell, Advisor
Allen Samarel, Loyola University Medical Center

ACKNOWLEDGEMENTS

I thank my thesis committee: Dr. Solaro, Dr. Samarel, and especially my mentor and advisor Dr. Russell. They have provided me with the encouragement, enthusiasm, and support to accomplish my goals and learn a little bit about myself in the process.

I also thank the Russell Lab members past and present who have provided me with companionship, insight, and laughter. Furthermore, I am especially grateful to Chad Warren whose guidance and expertise has been invaluable in completing this project.

Finally, I thank my family and friends who have been a continuous source of strength and love throughout this entire process.

ERS

TABLE OF CONTENTS

LIST OF TABLES

LIST OF FIGURES

LIST OF ABBREVIATIONS

2DGE	Two-dimensional gel electrophoresis
caPKC-ε	Constitutively active protein kinase C epsilon
CapZ	F-actin capping protein Z
DAG	Diacylglycerol
DMEM	Dublecco's Modified Eagle's Medium
dnPKC-ε	Dominant negative protein kinase C epsilon
ECM	Extracellular Matrix
ET-1	Endothelin-1
FRAP	Fluorescence recovery after photobleaching
GFP	Green fluorescent protein
IEF	Isoelectric focusing
MOI	Multiplicity of infection
NRVM	Neonatal rat ventricular myocyte
PBS	Phosphate buffered saline
PE	Phenylephrine
PKC	Protein kinase C
PLC	Phospholipase C
PTM	Post-translational modification
RACK	Receptor for active C-kinase
SDS	Sodium dodecylsulfate

SUMMARY

The heart is exquisitely sensitive to mechanical stimuli and adapts to increased demands for work by enlarging the cardiomyocytes through a hypertrophic response. It does this by increasing the proteins in the contractile units named sarcomeres. The mechanisms of sarcomeric remodeling in hypertrophy are complex and not entirely known; however, it is clear that mechanical deformation is at the genesis of this response. Mechanical strain triggers a signaling cascade within the cardiomyocyte resulting in post-translational modifications and concomitant alterations of the binding dynamics of proteins. Therefore, the goal of this study was to investigate the alterations in protein-protein binding dynamics and the post-translational profile of an important sarcomeric protein in response to mechanical strain.

Previous studies have demonstrated an alteration of F-actin capping protein (CapZ) binding dynamics and protein kinase C-ε (PKC-ε) dependence in response to hypertrophic stimulation. The specific hypothesis tested here is that CapZ undergoes a PKC-ε dependent post-translational modification that affects its actin binding dynamics in response to mechanical strain.

To test this hypothesis, neonatal rat ventricular myocytes were subjected to 10% mechanical strain at 1 Hz for 1 hour. To examine the role of PKC-ε on binding dynamics of CapZ, cells were infected with adenoviruses expressing dominant-negative or constitutively active PKC-ε prior to mechanical strain. Isoform specific CapZ binding rates were assessed by fluorescence recovery of

green fluorescent protein (GFP) after photobleaching using adenoviruses expressing wildtype GFP-CapZβ1 or GFP-CapZβ2.

Mechanical strain increased dissociation rates for CapZβ1 (196%, $p < 0.05$) above resting controls. Additionally, constitutively active PKC-ε increased the CapZß1 dissociation rate significantly (176%, $p < 0.05$) and dominant negative PKC-ε abrogated the effects of strain. No significant alterations in binding dynamics were observed for CapZβ2 after stimulation with mechanical strain or regulation of PKC-ε.

The isoform specific post-translational profile of CapZ was investigated with quantitative two-dimensional gel electrophoresis following mechanical strain and PKC-ε regulation. Two-dimensional western blotting identified two post-translational modifications of CapZβ1 and one modification of CapZβ2. Mechanical strain significantly increased the doubly modified form of CapZβ1 (117%, $p < 0.05$) while addition of dominant negative PKC-ε with mechanical strain reversed this effect. Constitutively active PKC-ε significantly increased the singly modified form of CapZβ1 (124%, $p < 0.05$). Neither mechanical strain nor PKC-ε regulation had any significant alteration on the post-translational profile of CapZβ2.

Taken together, these data strongly suggest that mechanical strain produces post-translational modifications of CapZβ1 but not of CapZβ2 through a PKC-ε dependent pathway. Furthermore, because constitutively active PKC-ε is able to recapitulate the binding dynamic alterations of mechanical strain and does not produce a similar post-translational profile of CapZβ1, additional

signaling pathways must also be operative. Mechanical strain may initiate PKC-ε dependent signaling pathways that converge on CapZ to alter actin filament capping dynamics and ultimately lead to cell remodeling and cardiac hypertrophy.

I. INTRODUCTION

A. Physiological and pathological cardiac remodeling

The heart is exquisitely sensitive to mechanical, hemodynamic, and hormonal stimuli, and adapts to increased demands for work by remodeling the cardiomyocytes though a hypertrophic response. Globally, this leads to increases in muscle mass, and if pathological cues are present, to disorganization of the contractile unit and apoptosis of the cell (Hunter *et al.,* 1999). At the cellular level, cardiomyocytes respond to mechanical strain and are able to remodel both their size and shape (Cooper *et al.,* 1990; Russell *et al.,* 2000).

In elite athletes, as the mechanical demands on the heart increase, sarcomeres are added both in parallel and series resulting in remodeling that increases both the width and length of the cells and ventricle while maintaining cardiac function (Pluim *et al.,* 2000). When these mechanical cues are pathological, as in situations of underlying disease, the cells remodel disproportionally. In situations with increased preload, the cells preferentially add sarcomeres in series, resulting in long, thin cells, and an enlarged, but thin heart. Conversely, in situations with increased afterload, the cells remodel to generate more force by adding sarcomeres in parallel, resulting in thick, short cells and heart.

The hypertrophy that occurs in pathological situations is believed to be initially adaptive, and helps the heart regain cardiovascular homeostasis. This is beneficial as it prevents the heart from experiencing extreme wall stresses while maintaining proper circulation and tissue perfusion (Grossman *et al.,* 1975). Over

time however, this compensatory process becomes maladaptive, and owing to a positive feedback loop, the heart becomes increasingly inefficient and unable to maintain homeostasis, and eventually is no longer able to meet the demands of the organism which results in death.

The remodeling that occurs in cardiomyocytes is primarily achieved through modifying the actin cytoskeleton, and myosin thick filaments composing the contractile units. Hypertrophic cytokines such as endothelin-1, angiotensin II, insulin growth factor I, and others that lead to $G\alpha_q$ activation can lead to both long term modifications in gene expression and short term modifications in the proteome (Hunter *et al.,* 1999). Mechanical strain is also sensed and transduced into biochemical hypertrophic stimuli through mechanisms which continue to be elucidated, but may converge on similar pathways with the cytokines. These pathways may subtly or overtly modify the actin cytoskeleton leading to changes in subcellular dynamics and structure. Indeed, modifications that affect actin attachment to the Z-disc lead to dilated cardiomyopathy and heart failure (Olson *et al.,* 1998; 2000). The localized changes in binding affinity and rate may lead to global remodeling of the actin cytoskeleton to meet the mechanical and biochemical cues present.

During this decompensated phase, the heart undergoes many changes at the molecular, cellular, and tissue levels. Cardiac signaling pathways are altered, cytoskeletal organization becomes disrupted, cell-cell interaction is modified, and cell viability decreases (de Tombe *et al.,* 2000). It is the integration of all these modifications that leads to the inefficiency, and ultimately, the failure of the heart.

B. Mechanotransduction and the Z-disc

Understanding the mechanisms through which cardiomyocytes sense and respond to biomechanical stress is of prime importance to the development of a molecular basis of heart failure. The cardiomyocytes experience changes in stress and strain through every cardiac cycle, which have proven to be great regulators of gene transcription and post-translational modification that alters cell shape and function. Furthermore, these stresses and strains are generated both internally by contractile proteins, and externally through cell-cell and cell-matrix interactions. Cells within the heart are constantly remodeling through a process involving gene transcription, protein translation, and protein post-translational modification. Gene regulation and protein translation within the heart occupy a much longer time scale than post-translational modifications, and are unable to respond quickly to acute stresses and strains. Because the heart is constantly being challenged mechanically, it relies upon post-translational modification of proteins to sense and respond appropriately to the external stressors. The mechanism through which the cardiomyocytes sense and respond to acute mechanical strain, including beat-to-beat strain, remains largely unknown. The Z-disc lattice structure is altered by the mechanical forces of contraction arising from actin-myosin interactions making it a possible site as a mechanosensor.

Due to the abundance of actin within a cardiomyocyte and its role in contraction, cellular processes, and maintenance and remodeling, the cell must regulate the polymerization and depolymerization of actin filaments. Furthermore, the concentration of actin capping protein at the Z-disc, and its ability to modulate

actin polymerization and stability, suggests that CapZ may be an important protein in the mechanosensory pathway. The first studies of CapZ conclusively demonstrated its ability to modify the length of existing actin filaments, and prevent reformation of an actin network after disruption (Maruyama, 1966).

Internally, cardiomyocytes generate force through their contractile filaments that are anchored together by an abundance of proteins organized at the Z-disc. The Z-disc anchors parallel, actin containing thin-filaments by tight cross-linking with α-actinin. Classically, α-actinin was believed to be the major component of the Z-disc, but recent studies have shed light on many other proteins that interact to form the Z-disc ultrastructure. The overall architectural complexity of the Z-disc means that it could function not only as a mechanical joint, but also as a signaling complex.

Externally, cardiomyocytes are bound to their extracellular matrix through costameres, which form a physical attachment internally via the Z-disc and externally via integrins at the focal adhesion. Furthermore, many signaling molecules and cytoskeletal proteins localize to the Z-disc, providing the cell with both biochemical and mechanical sensors to external stress. Mechanosensitive ion channels supply one possible biochemical link between the cytoskeleton and extracellular matrix, however this does not fully address mechanotransduction at the costamere and Z-disc. It has been proposed that mechanical strain physically deforms proteins, thus changing the affinity of binding sites, which alters the association between signaling molecules and their effectors (Riveline *et al.,* 2001). Many groups have identified proteins in cardiomyocytes that localize to

the Z-disc, and alter binding affinity through a stretch-dependent pathway, such as F-actin capping protein (CapZ) and protein kinase C epsilon (PKCε) (Disatnik *et al.,* 1994; Zhu *et al.,* 2000; Pyle *et al.,* 2004).

C. CapZ structure and function

The F-actin capping protein is an essential protein involved in actin cytoskeletal remodeling. CapZ was first discovered in the 1960s by Maruyama and colleagues and was called β-actinin (Maruyama *et al.,* 1965; 1966; 1977). These studies demonstrated that increasing the concentration of CapZ decreased the length of F-actin polymers after sonication and prevented polymerization of G-actin. After sonication and dispersion of F-actin polymers, Asakura *et al.,* discovered that there was a fast recovery to the original state that could be slowed or prevented by addition of CapZ at various time points though the mechanism through which this occurred was unknown (Asakura *et al.,* 1961, 1963). CapZ continued to be studied and was finally purified to homogeneity in 1980 which led to the discovery that it is composed of two major polypeptides approximately 30kDa in size, that pair to cap the barbed end of actin filaments (Isenberg *et al.,* 1980).

CapZ is a heterodimer composed of an alpha and a beta subunit. Vertebrates contain three alpha isoforms that are encoded from three individual genes, and three beta isoforms that are generated through alternative splicing. The α1 and α2 isoforms are found throughout many tissues though their expression varies widely, and the α3 isoform is specific to the testis. In cardiac

tissue, the ratio of α1 to α2 is approximately 1.2:1 (Hart *et al.,* 1997). The different biochemical, cellular, and functional roles of each α isoform continues to be elucidated.

The β1 and β2 isoforms are also found throughout various tissues, and similarly to the α3 subunit, the β3 isoform is specific to the testis. Because each β isoform is generated through alternative splicing, they contain great sequence similarity (Fig 1B). The β1 and β2 isoforms vary only in their COOH-terminal ends (β1 - 31 amino acids, β2 – 26 amino acids) and β3 is identical to β2 with the addition of 29 amino acids at the NH_2 terminal end (Hug *et al.,* 1992; Schafer *et al.,* 1994; von Bulow *et al.,* 1997). Although the protein sequences are extremely similar, the β1 and β2 isoforms have distinct functions and biochemical roles. The evidence for their differing roles includes high conservation among vertebrate species, tissue specificity, and well-defined subcellular location (Schafer *et al.,* 1994). The β1 isoform has been shown to be highly expressed in muscle tissue with a ratio of β1 to β2 approximately 2:1, whereas the β2 isoform is predominately expressed in non-muscle tissue (Schafer *et al.,* 1994; Hart *et al.,* 1997, Hart *et al.,* 1999). Furthermore, the β1 isoform localizes to the Z-disc in striated muscle, whereas the β2 isoform localizes to the intercalated discs and plasma membrane (Schafer *et al.,* 1994). Overexpression of the β1 isoform in cardiac tissue causes disruptions in the intercalated discs, and overexpression of the β2 isoform causes severe malformations of the myofibril architecture (Hart *et al.,* 1999).

The CapZ α/β complex is shaped liked a mushroom (Yamashita *et al.,* 2003). Both subunits have similar secondary structure, and are arranged such that the molecule has a pseudo-two-fold axis of rotational symmetry (Fig. 1A) (Yamashita *et al.,* 2003). The COOH-terminal ends of both of the α and β subunits have amphiphilic α-helices which bind actin on the hydrophobic side (Barron-Casella *et al.,* 1995; Yamashita *et al.,* 2003; Wear *et al.,* 2003). The hydrophilic side of the COOH-terminal ends has isoform specific charge distributions and may be involved in isoform specific recognition of target ligands (Yamashita *et al.,* 2003). Thus, the tentacles present on CapZ are hypothesized to allow binding of both actin and a specific target protein. The separation of the two C-terminal ends ensures that each tentacle binds a single actin monomer at the end of filamentous actin (F-actin). This property explains the inability of CapZ to bind monomeric actin (G-actin) and its strong association with F-actin. Furthermore, studies have shown that when CapZ is bound to F-actin by only its β-tentacle, the molecule is able to 'wobble' and thus exposes additional actin and target binding sites to other molecules (Kim *et al.,* 2007). Although it was initially believed that the β tentacle was the only mobile region on CapZ (Wear *et al.,* 2004), new data suggest that CapZ is intrinsically flexible allowing it to interact with the barbed-end of actin in both a high and low affinity state (Taketa *et al.,* 2010).

Wild type CapZ binds F-actin with sub-nanomolar affinity (~0.1nM) and it has been shown through multiple studies that the C-terminal domain is necessary for high-affinity actin binding (Wear *et al.,* 2003; Kim *et al.,* 2010). Any

modifications and mutations that affect the C-terminal ends may greatly reduce the affinity of CapZ to F-actin (Kim *et al.,* 2010). CapZ was believed to bind to actin in a two step model whereby electrostatic interactions with the α subunit dictate the on-rate and hydrophobic interactions of actin with the β subunit dictate the off-rate (Narita *et al.,* 2006). Based on affinity and x-ray crystallography studies, an improved mechanism by which CapZ binds actin is as follows. (i) Basic residues on the α tentacle interact electrostatically with the barbed end of actin (ii) A conformational change of CapZ to a high-affinity form occurs (iii) supportive binding of the β tentacle strengthens the association (Kim *et al.,* 2010). Thus, a factor or mechanism that disturbs any of the binding or unbinding steps may inhibit the capping ability of CapZ or promote uncapping.

A.

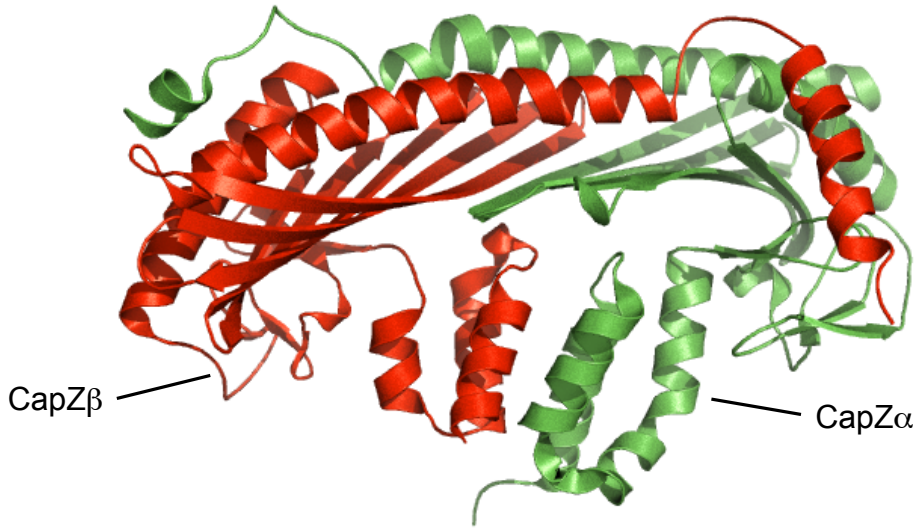

B.

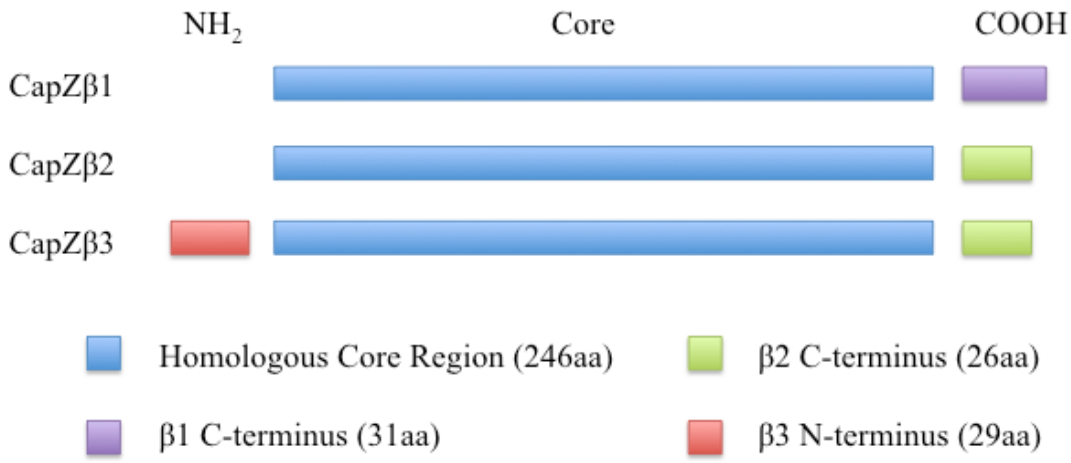

Figure 1. CapZ secondary structure and sequence conservation.
(a) Ribbon diagram of CapZα/β heterodimer. CapZα isoform is depicted in green; CapZβ isoform is depicted in red. (b) CapZβ isoform sequence comparison demonstrates a 246aa conserved core region of all isoforms; a unique 31aa C-terminal extension of the β1 isoform; a common 26aa C-terminal extension of β1 and β2 isoforms; a unique 29aa N-terminal extension of the β3 isoform.

D. Protein kinase C function and regulation

The protein kinase C (PKC) family of enzymes transduces many signal pathways within the cell ranging from lipid hydrolysis to mechanotransduction. The wide-ranging affect of protein kinase C may be due in part to the many pathways that lead to its activators diacylglycerol (DAG) and phorbol ester (Newton, 1995). Furthermore, protein kinase C activation requires phosphatidylserine that is found exclusively on the cytoplasmic side of the cell membrane (Nishizuka *et al.,* 1986). Extensive studies have determined the structure of the protein kinase C family enzymes that contain an N-terminal regulatory region and a C-terminal catalytic region within four conserved domains C1-C4 (Coussens *et al.,* 1986). The C1 domain contains a cys-rich region responsible for the diacylglycerol and phorbol ester binding site which is immediately flanked by an autoinhibitory region (House *et al.,* 1987). The C2 domain contains the recognition site for lipids and Ca2+ binding. The C3 and C4 domains form the functional site of PKC which bind ATP and substrate (Taylor *et al.,* 1994). The regulatory and catalytic domains of PKC are separated by a hinge region that becomes proteolytically available when the enzyme is membrane bound, and once freed from the regulatory domain PKC becomes constitutively active (Inoue *et al.,* 1977). Three families of PKC have been identified to date, containing a total of 11 isozymes. The 'classical' isoforms (α, βI, βII, and γ) are regulated by calcium, DAG, and phosphatidylserine; the 'novel' isoforms (δ, ε, η, ϕ, and μ) are regulated by DAG, and phosphatidylserine; and

the ‘atypical’ isoforms (ζ and λ) that require only phosphatidylserine for activation.

It has long been understood that phospholipase C (PLC) hydrolyzes phosphatidylinositol-4,5-biphosphate (PIP2) into inositol 1,4,5-triphosphate (IP3) and DAG through activation of $G_q\alpha$ receptors in the classically described IP3/DAG pathway. This pathway in turn leads to the activation of PKC, which can modify myriad cytoplasmic proteins through phosphorylation of serine or threonine residues. Binding of DAG with the C1 domain, and additionally the C2 domain in the novel isoforms, which also binds a class of proteins called receptors for activated PKC (RACK), contribute to the localization and activation of PKC (Mellor *et al.,* 1998). Furthermore, studies have shown that the binding between the C1 domain and DAG does not necessitate translocation to the plasma membrane, but that translocation may also be dependent on the selective recruitment of DAG effectors (Diaz-Flores *et. al,* 2003). PKC-ε has been shown to be important in regulating cardiac contractility and is translocated through a distinct mechanism to the Z-disc.

The novel PKC isoform ε has been shown to be important in modulating cardiac contractility and remodeling. When activated, PKCε translocates to the Z-disc and can be observed to have a striated, sarcomeric appearance in myocytes (Disatnik *et al.,* 1994). The upstream signaling cascade involved in the activation of PKC-ε takes between 5-20 minutes, though the steps and binding partners in this cascade remain unknown (Huang *et al.,* 1997). The long time involved in translocation of PKC-ε to the Z-disc suggests intramolecular

rearrangement of its binding partners and surfaces at the Z-disc (Robia *et al.,* 2001). It has also been suggested that the regulatory binding region of PKC-ε is obscured until stimulation (Dorn *et al.,* 1999). The identities of all the binding partners of PKC-ε at the Z-disc remain unknown, though some have suggested Cypher-1 and enigma homologue protein, PDZ domain containing proteins that also bind α-actinin, several RACKs, and F-actin (Mochly-Rosen, 1995; Prekeris *et al.,* 1996; Zhou *et al.,* 1999; Nakagawa *et al.,* 2000). Furthermore, the PKC-ε activators DAG and phorbol ester increase the enzyme's membrane affinity by contributing to a hydrophobic surface of the C1 domain of PKC (Zhang *et al,* 1995). Interestingly, in transgenic models of CapZ downregulation, PKC dependent regulation of myofilament function is abolished, and activated PKC-ε and PKC-β binding to the myofilament is diminished (Pyle *et al.,* 2002). In addition, treatment of cardiomyocytes with the hypertrophic cytokine endothelin-1 or the α1-adrenergic receptor agonist phenylephrine caused an alteration in CapZ dynamics through a PKC-ε and PIP2 dependent pathway that decreased the affinity of CapZ to F-actin (Hartman *et al.,* 2009).

Taken together, the abundance of PKC anchoring proteins at the cardiac Z-disc indicates a significant role for both the Z-disc and CapZ in PKC dependent signaling pathways.

E. Fluorescence recovery after photobleaching to study live cell dynamics

Fluorescence recovery after photobleaching (FRAP) is an extremely useful technique to study *in vitro* protein-protein interactions and dynamics. In FRAP, fluorescent molecules are irreversibly bleached in an area of interest, and the rate of recovery of fluorescence is indicative of how quickly unbleached fluorescent molecules move back into the area and structural complexes. The rate at which these molecules move into the area of interest is influenced by the subcellular niche, which affects diffusion, transport, and protein-binding interactions. The information obtained from molecular motilities can be used to determine rates of cellular diffusion in specific subcellular compartments, reveal dynamic structures and complexes in stimulated and non-stimulated states, and measure and identify binding interactions. Furthermore, FRAP is ideally suited to studying biological processes that occur on a time-scale of seconds to minutes.

When a fluorescent tag, such as GFP, is bound to a protein of interest and expressed within a cell, both qualitative and quantitative information can be obtained. Qualitatively, the shape of the fluorescent recovery curve can offer insight into the mechanisms of protein mobility. Three basic curve shapes can be obtained as shown in Fig. 2 and relate to mechanisms dominated by (A) pure diffusion, (B) diffusion dependent, and (C) two-binding state recovery.

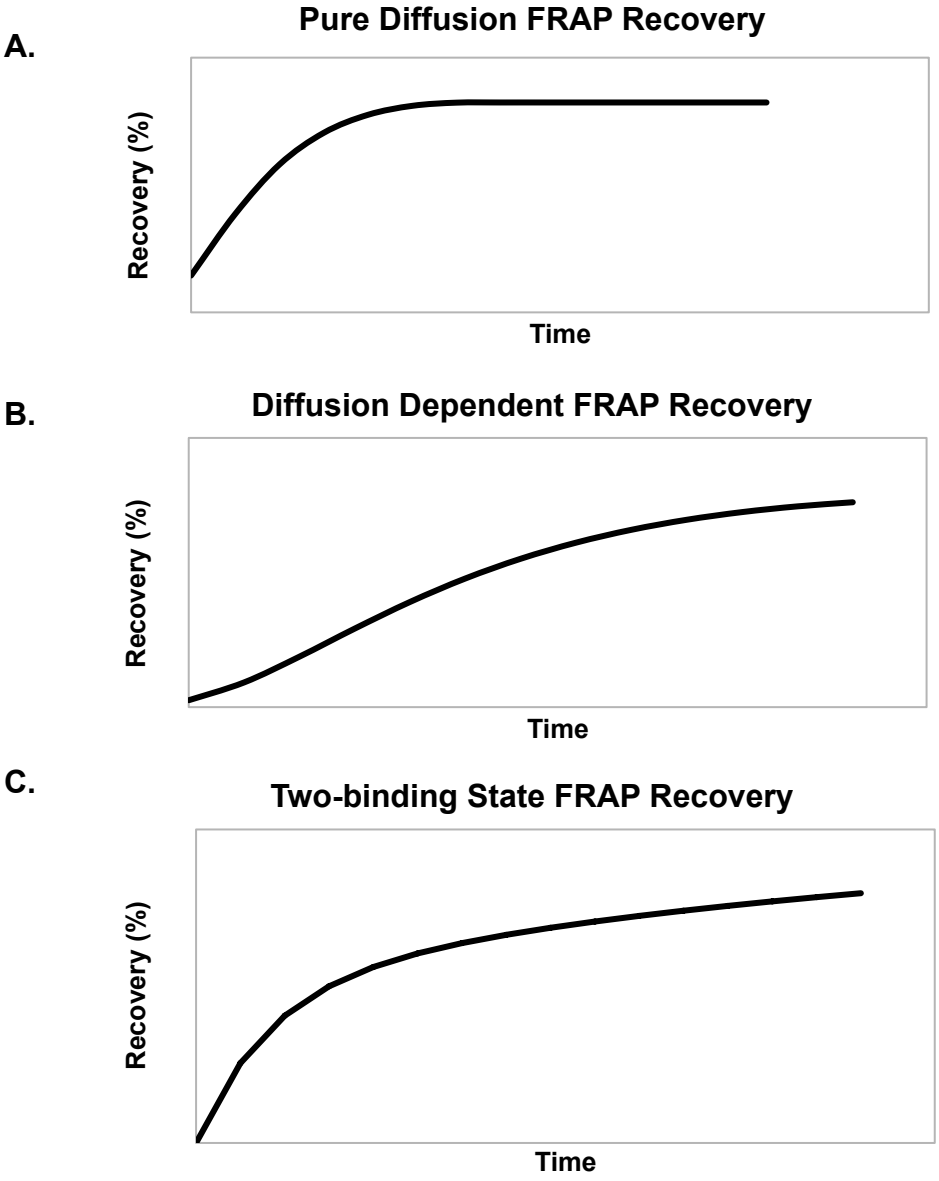

Figure 2. Characteristic FRAP recovery curves. Average FRAP recovery intensity within the bleach spot is plotted as a function of time, yielding the three characteristic FRAP curves based upon binding dynamics. (a) Curve profile represents pure cellular diffusion with no binding interaction, and yields a high initial rate of recovery followed by a stable signal due to the rapid kinetics of diffusion. (b) Curve profile represents diffusion-dependent FRAP recovery, and yields a curve with a steady increase in fluorescence after photobleaching. (c) Curve profile represents diffusion-independent FRAP recovery with two-binding states, and yields a curve with an initial high rate of recovery from the fast mobile fraction, followed by a lower rate of increase in fluorescence due to the slow mobile fraction.

The first curve (Fig. 2A) is generated when most fluorescent molecules are free and do not interact with the subcellular milieu. The second curve (Fig 2B.) is generated when the binding process of proteins is much faster than that of diffusion, resulting in a slowed diffusion rate. The third curve (Fig. 2C) is generated when diffusion occurs much more rapidly than binding, and is not detected in the FRAP recovery, such that the curve represents protein-binding interactions alone. Quantitatively, equations can be used to model each of the curve shapes, and important information about the rate and equilibrium of the protein interactions can be extracted. The first two curve shapes can be fit using an equation for diffusion that has been extensively studies and is as follows:

$$I_{frap}(t) = e^{\frac{-\Gamma_D}{2t}}\left[I_0(\frac{\Gamma_D}{2t}) + I_1(\frac{\Gamma_D}{2t})\right] \quad (1)$$

Where,

$$\Gamma_D = \frac{w^2}{D_f} \quad (2)$$

Where I_{frap} is the intensity of the spot, w is the radius of the bleach spot, D_f is the calculated diffusion constant, and t is time. This formula is used to model the FRAP recovery of free GFP. The third curve shape can be characteristically quantified using the following formula for two binding states:

$$I_{frap}(t) = 1 - C_1 e^{-k_{1off}t} - C_2 e^{-k_{2off}t} \quad (3)$$

Where C_1 and C_2 are the equilibrium concentrations for the fast and slow binding states respectively, and K_{1off} and K_{2off} are the off-binding rates for the fast and slow reactions respectively. When the empirical data is fitted to these curves using non-linear regression, valuable information such as the off-rate and equilibrium constants of the protein-protein interactions can be obtained.

A number of considerations must be taken to ensure accurate and reproducible results which include: cell preparation, choice of microscope and optical settings, number and duration of images taken before and after bleaching, size of the region of interest, and laser power used for bleaching and data acquisition (McNally, 2008). When used properly, FRAP allows *in vitro* examination of protein interactions and can be used to study and model the biophysical conditions present.

F. Techniques to study *in vivo* and *in vitro* post-translational modifications

Due to the importance of post-translational modification of proteins within the cell, several techniques have been developed that allow both the identification and quantification of modifications *in vivo* and *in vitro.* One of the most useful techniques is two-dimensional gel electrophoresis (2DGE). At its most basic, 2DGE exploits the ability of zwitterionic amino acids to vary their charge based upon the surrounding pH of the solvent. Post-translational modifications add, remove, and modify the functional groups attached to the residues within a protein and alter its ability to carry a net charge under varying

pH. When unmodified proteins are subjected to an electrical current, the negatively charged molecules migrate towards the anode. When a stable increasing pH gradient is established between the anode and cathode, as proteins migrate towards the anode (+) the zwitterionic amino acids acquire more positive charge from the hydronium ions and migration slows. Eventually, enough hydronium ions protonate the amino acids of the protein and all net charge is removed. The pH at which the net-charge of the protein is zero is called the isoelectric point (pI). Post-translational modifications may affect the pI of a protein by modifying the functional groups, or the ability of the groups to acquire charge. For example, a post-translational modification of phosphorylation will add a negative phosphate ion to the molecule, and will thus lower the pI of the molecule. Therefore, adding a complex mixture of post-translationally modified proteins into an immobilized pH gradient and applying an electric current, one is able to separate the various modifications of proteins by their pI. Following this separation of proteins by pI, the proteins are then subjected to conventional one-dimensional SDS-polyacrylamide gel electrophoresis to separate proteins by size. This technique is called two dimensional gel electrophoresis and was first described in the 1980's. (Gorg *et al.,* 1988). Quantitative western blotting from this technique allows probing of specific proteins and may provide evidence of post-translational modifications.

While 2DGE is an extremely useful technique to observe and test post-translational modifications, it cannot always provide information about which post-translational modification is occurring and cannot easily identify the site of

modification. To meet these limitations, mass spectrometry can be used to conclusively identify the sites and types of post-translation modification. Briefly, proteins can be digested into peptides through enzymatic degradation, vaporized and ionized, and separated in a mass spectrometer by their mass-to-charge ratio. The ions that are produced can then be quantitatively measured, and fragmented again to monitor possible post-translational modifications. This process is called tandem mass spectrometry. The second fragmentation process often cleaves the post-translational modification from the amino acid backbone and results in an ion with a different mass-to-charge ratio. Many post-translational modifications have been well characterized and documented so that a mass spectrometer can distinguish between the specific types of modification on an individual peptide. Furthermore, as the ions are scanned for post-translational modifications, the identity of each peptide fragment and its parent protein can be determined. This provides the ability to analyze complex samples and determine both protein identities and modifications in a single sample. This technique is especially useful when coupled with other proteomic techniques such as co-immunoprecipitation to identify binding partners of proteins of interest.

Used together, two dimensional gel electrophoresis and mass spectrometry are extremely valuable tools that provide insight into the complex mechanisms of post-translational modification both *in vivo* and *in vitro.*

II. METHODS

A. Neonatal rat ventricular myocyte primary cell culture

Animal experiments were performed ethically according to Institutional Animal Care and Use Committee and NIH guidelines.

Briefly, ventricular myocytes were isolated from the hearts of 1-3 day old Sprague-Dawley rats (Harlan, Indianapolis, IN). Hearts were excised and placed in ice-cold Moscona's saline (136.8mM NaCl, 28.6mM KCl, 11.9mM $NaHCO_3$, 9.4mM Glucose, 0.08mM NaH_2PO_4, ph 7.4) and rinsed three times. The hearts were then placed in ice-cold KRBI solution (118.4 mM NaCl, 4.7mM KCl, 23.8mM $NaHCO_3$, 2.4mM MgSO4, 1.5mM KH_2PO_4, pH 7.4) and rinsed twice. The ventricles were then trimmed free and minced on ice with dissecting scissors.

Cells were then dissociated with a crude collagenase type II solution (1000U/heart in saline, Worthington Biochemical Corporation) in a 37°C shaking bath. Digestion supernatant was drawn every 10 minutes for 6-7 sequential digestions, and placed in a Dulbecco's Modified Eagle's Medium/Nutrient Mixture F-12 HAM without L-glutamine (DMEM)/10% FBS solution on ice to halt further enzymatic digestion. Digestions were then consolidated, and cells resuspended in complete media (DMEM, FBS 5% (v/v), BSA 0.1% (w/v), standard amino acid concentrations, and pencillin/streptomycin/amphotericin B solution (10μl/ml)). The cell suspension was then plated for 1hr to reduce non-myocyte contamination.

Cells were resuspended in serum free media (PC-1, Lonza) and plated on corona treated (30 seconds) and fibronectin coated (25μg/ml) FlexCell© silicone

membranes (200,000 cells/cm$^{2)}$. Cells were left undisturbed for 24 hrs in a 5% CO_2 incubator. Unattached cells were removed by aspiration and serum-free media was replenished. Cells were left undisturbed 24hrs prior to the experiment.

B. Adenoviral constructs and transfection

Recombinant adenoviruses for CapZβ1-GFP, GFP-CapZβ2-GFP, constitutively active PKCε (caPKCε), and dominant negative PKCε (dnPKC-ε) were kindly provided by Dr. Allen Samarel (Loyola University Chicago Stritch School of Medicine, Maywood, IL). Cardiomyocytes were infected with CapZβ1 (MOI 20), CapZβ2 (MOI 20), caPKCε (MOI 100), or dnPKC-ε (MOI 250) for 60min at 37°C diluted in DMEM/M199 (4:1) solution (Strait *et al.,* 2001; Hartman *et al.,* 2009). Viral medium was then replaced with virus-free medium, and cells were left undisturbed for 24hrs.

C. Mechanical strain

Cyclic mechanical strain was generated with a Flexcell ® Strain Unit (Model FX-4000™, Flexcell International Corporation, Hillsborough, NC). Cells were stretched at 10% elongation biaxially (Colombo *et al.,* 2008), at 1Hz sinusoidally, for 1 hour in non-serum media (*Fig*. 3). Strain magnitude, time, and waveform were user-assigned to the system that controls vacuum pressure (Flex Central, Flexcell International Corporation, Hillsborough, NC) to deliver calibrated strain values to available elastic substrates housed in the incubator.

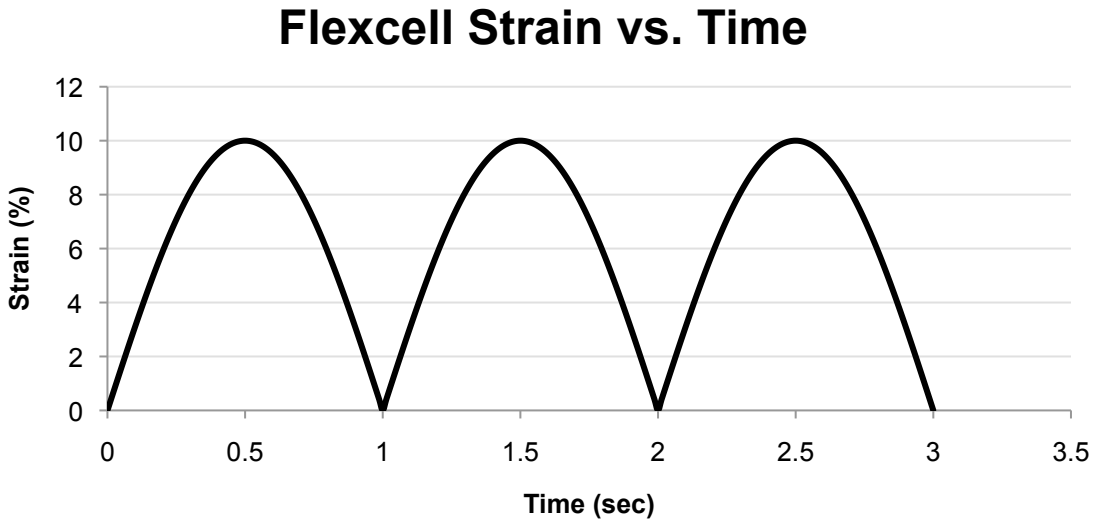

Figure 3. Mechanical strain profile. Cells are subjected to a stretch and relaxation cycle at 1 Hz with an approximate 10% maximum strain for 1 h on a biaxial stretch system.

D. Fluorescent recovery after photobleaching and analysis

One to ten beating and well-striated cells (as evidenced by CapZ-GFP tag) were randomly selected for each FRAP study immediately after stretching. The GFP fusion protein was irreversibly bleached by laser excitation (488ηm) at full power in a uniform square region of interest (36μm^2) lying midway between the cell nucleus and periphery. The intensity of the region of interest (I_{frap}) was observed both before (t_0) and immediately after (t_1) bleaching, and intermittently every 2 minutes until the end of the 15 minute study. A control region within the cell (I_{ref}) and outside (I_{back}) were also recorded to ensure accurate results. Images were analyzed using Zeiss Imaging Browser. Intensities at any given time were normalized using the following formula (Phair *et al*, 2004):

$$I_{frap}(t) = \frac{I_{ref}(t_0) - I_{back}(t_0)}{I_{ref}(t) - I_{back}(t)} \cdot \frac{I_{frap}(t) - I_{back}(t)}{I_{frap}(t_0) - I_{back}(t_0)} \qquad (4)$$

Plotted intensity values are given as a percentage of the difference between $I_{frap}(t_0)$ and $I_{frap}(t_1)$. Curves were fitted to the equation (3) using non-linear regression in OriginPro (OriginLab, Northampton, MA). Only curves fit with a coefficient of determination (R^2) greater than or equal to 90% and successful convergence were used. Average kinetic constant off-rates (K_{FRAP}) were calculated using the following formula:

$$K_{frap} = C_1 \cdot K_{off1} + C_2 \cdot K_{off2} \qquad (5)$$

E. Two-dimensional gel electrophoresis

Immediately following mechanical strain, cells were placed on ice and lysed using ice cold MF buffer (75mM KCl, 10mM Imidazole, 2mM $MgCl_2$, 2mM EDTA, 1mM NaN_3) containing protease and phosphatase inhibitors (Sigma, St. Louis, MO). Pellet was then resolubilized in urea-thiourea-chaps (UTC) buffer (8M Urea, 2M Thiourea, 4% Chaps). Total protein concentration was measured using the Bradford method with crystalline bovine serum albumin as standard. 100μg of protein was precipitated using a 2D Clean-up Kit (GE Healthcare, Burr Ridge, IL) and resuspended in 16μl of UTC buffer. 324μl of isoelectric focusing buffer (800μl UTC, 8mg DTT, 8ul Destreak, 4μl ampholytes) was added to each sample.

Samples were loaded into the isoelectric focusing cell and set with: passive rehydration 10-16hrs, 250v rapid – 15 minutes, 10000V slow – 2 hours, 10000V rapid – 55,000 volt-hrs, 500V hold. pH 4-7 IEF strips were loaded over samples and covered with mineral oil. IEF cell was then run to completion.

First dimension IEF strips were then incubated with IEF EQ buffer (6M urea, 5% SDS (w/v), 30% glycerol (v/v)) containing 1% DTT for 10 minutes. Strips were then removed, rinsed, and incubated in IEF EQ buffer containing 2.5% Iodoacetamide for 15 minutes. Strips were then loaded on 12.5% SDS-polyacrylamide gels and run at 30mA per gel until dye front migrated off gel. Proteins were then transferred to a pre-wet polyvinylidene fluoride membrane and transferred using CAPS buffer at 20V for 70 minutes. Proteins were probed with antibodies: CapZβ1 (mAb 1E5.25.4, Developmental Studies Hybridoma

Bank, IA); CapZβ2 (mAb 3F2.3, Developmental Studies Hybridoma Bank, IA) and visualized using enhanced chemiluminescence (ECL+, Amersham, Arlington Heights, IL) and quantified by optical densitometry.

F. Immunoprecipitation and mass spectrometry

The isolated ventricles from 10 hearts of 1-3 day old Sprague-Dawley rats were excised and flash frozen in liquid nitrogen. The hearts were then homogenized on ice using a dounce homogenizer in MF buffer (75mM KCl, 10mM Imidazole, 2mM $MgCl_2$, 2mM EDTA, 1mM NaN_3) containing protease and phosphatase inhibitors (Sigma, St. Louis, MO). The protein was then precipitated and resolubilized in UTC buffer (8M Urea, 2M Thiourea, 4% Chaps). Total protein concentration was calculated using the Bradford method. 1mg of protein was then resolubilized in 40μl of UTC buffer for each immunoprecipitation. 50μl of Protein G conjugated Dynabeads (Invitrogen, Grand Island, NY) was incubated with 10μl of CapZβ1 antibody (mAb 1E5.25.4-c, Developmental Studies Hybridoma Bank, IA) with rotation for 15 minutes at room temperature. The antibody was then crosslinked to the beads using 5mM BS^3 (Thermo Fisher Scientific, Rockford, IL). The 40μl sample in UTC buffer was then diluted 30-fold with standard IP buffer (20mM Tris-HCl pH 7.4, 137mM NaCl, 1% Triton-X 100, 2mM EDTA) plus protease and phosphatase inhibitors. The sample was then incubated with the magnetic beads for 15 minutes at room temperature with rotation. The bound proteins were then eluted from the magnetic beads using 20μl of UTC buffer for 15 minutes at room temperature

with gentle rotation. Sample buffer was then added to the eluate and heated at 93°C for 7 minutes. The sample was then loaded on a 12.5% SDS-polyacrylamide gel and run at 30mA at 4°C until the dye front migrated off the gel.

For western blotting, the proteins were then transferred to 0.45 μm polyvinylidene fluoride membrane using CAPS buffer at 20V for 70 minutes. The blot was then probed with CapZβ1 antibody (mAb 1E5.25.4, Developmental Studies Hybridoma Bank, IA). For mass spectrometry, the gel was fixed with colloidal coomassie fixative (45% MeOH, 1% HoAC) and stained with colloidal coomassie (G-250 Biosafe Coomassie, Bio-rad, Hercules, CA). Gel bands were then excised, minced, and stored in coomassie fixative solution. Mass spectrometry services were provided by the mass spectrometry, metabolomics, and proteomics facility at the University of Illinois at Chicago Research Resource Center. Briefly, samples were extracted from the gel slices, digested using trypsin, and analyzed using a Thermo Scientific Orbitrap Velos Pro. Results were then analyzed using Scaffold (Proteome Software, Portland, OR).

III. RESULTS

A. GFP-CapZ localization

The localization of CapZ within the myocyte is an important regulator of cell remodeling. Previously, studies have shown that CapZβ1 localizes to the Z-disc and CapZβ2 localizes to the plasma membrane and intercalated discs (Schafer *et al.,* 1994). In order to study *in vitro* dynamics at the Z-disc accurately, localization of each GFP tagged CapZ isoform was necessary. In cardiomyocytes expressing GFP-CapZβ1, a strong association with staining for α-sarcomeric actinin was present (Fig. 4A). The striated pattern of GFP-CapZβ1 that overlays an identical pattern of α-sarcomeric actinin suggests that expression of the GFP-CapZβ1 fusion protein does not interfere with proper CapZβ1 localization to the Z-disc. A low level of background GFP-CapZβ1 is also observed, and suggests that there is a minimal amount of uncomplexed CapZβ1 within the cell.

Expression of GFP-CapZβ2 in cardiomyocytes demonstrates little localization with existing structures (Fig. 4B). It is noted that CapZβ2 has a dense localization at the plasma membrane, but also exists throughout the cytoplasm in a punctate pattern. The localization of CapZβ2 is consistent with prior findings (Schafer *et al.,* 1993) and indicates that the fusion protein does not interfere with proper CapZβ2 localization to the Z-disc.

A.

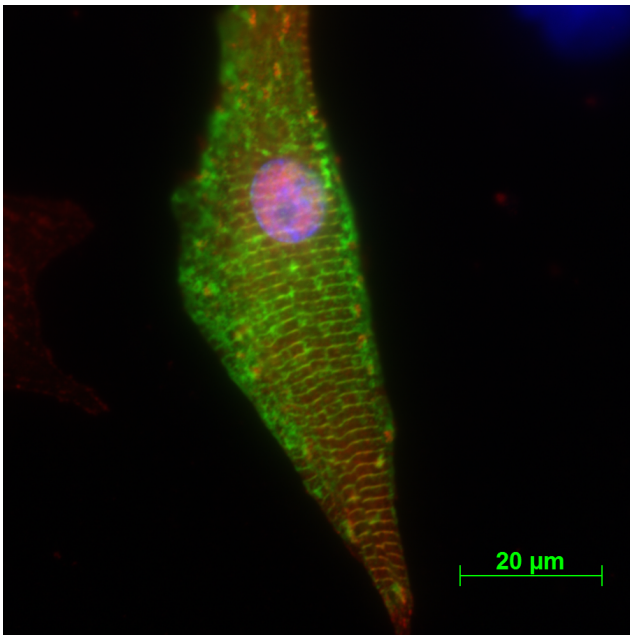

B.

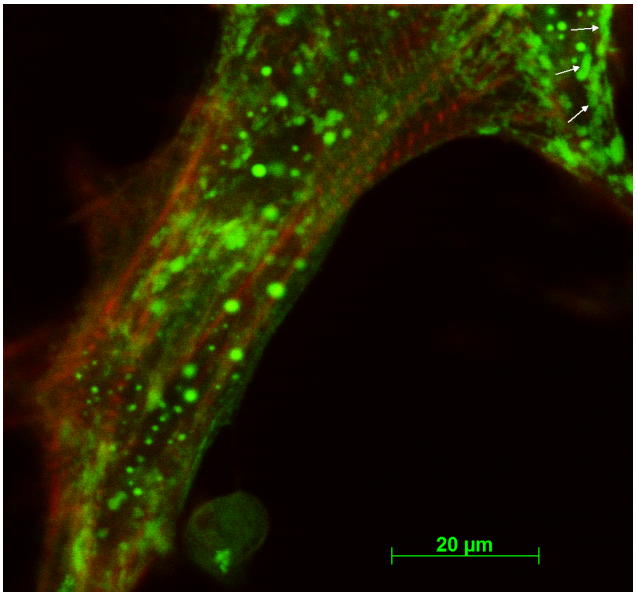

Figure 4. Localization of GFP-CapZ isoforms in cultured NRVM. NRVM were cultured for 48 h, infected with WT GFP-CapZβ1 or GFP-CapZβ2 for 1 h, and cultured for an additional 24 h, at which point they were fixed and subjected to staining with α-sarcomeric actinin. (a) Cells expressing WT GFP-CapZβ1 demonstrate localization at the Z-disc. (b) Cells expressing WT GFP-CapZβ2 demonstrate a punctate pattern of staining throughout the cytoplasm with increased staining at the plasma membrane (arrowheads).

B. CapZβ1 but not CapZβ2 actin-capping dynamics are altered by mechanical stress and PKC-ε expression

The rate of CapZ binding and unbinding within the cell were hypothesized to be an important regulator in cytoskeletal remodeling (Wear *et al.,* 2003). The FRAP recovery curves generated by bleaching CapZβ1 follow a standard two-binding model curve shape as previously described (Fig. 2). Non-stretched cardiomyocyte FRAP response recovery at 15 minutes was 46 ± 4%. Upon treatment of mechanical strain, CapZβ1 recovery at 15 minutes was 57 ± 6%. Non-stretched cells treated with caPKC-ε recovery at 15 minutes was 59 ± 7%. Finally, stretched cells treated with dnPKC-ε recovery at 15 minutes was 35 ± 5% (Fig. 5). The free GFP recovery profile characteristically displayed a free-diffusion binding curve as previously mentioned. Recovery at 15 minutes for GFP was 83 ± 5% (Fig. 5). The levels of recovery suggest altered binding affinity of CapZ for actin under each condition.

To measure binding rates quantitatively, every FRAP recovery curve for each condition was fit using the equation (3) and an average kinetic constant, K_{FRAP}, was generated using the equation (5). K_{FRAP} values for each of the conditions indicate altered binding dynamics of CapZβ1 after mechanical strain or treatment with caPKC-ε (Fig. 6A). Non-stretch control cells had a K_{FRAP} of $2.5 \cdot 10^{-3} \pm 2.3 \cdot 10^{-4} s^{-1}$ which was significantly different from a K_{FRAP} of $4.9 \cdot 10^{-3} \pm 5.6 \cdot 10^{-4} s^{-1}$ for stretched cells ($P < 0.01$, n=5). Additionally, non-stretched cells treated with caPKC-ε had a K_{FRAP} of $4.4 \cdot 10^{-3} \pm 5.1 \cdot 10^{-4} s^{-1}$ which was significantly different from non-stretched cells ($P < 0.05$, n=5) but not significantly different

from stretched cells. Stretched cells treated with dnPKC-ε had a K_{FRAP} of $2.2 \cdot 10^{-3} \pm 6.5 \cdot 10^{-4} s^{-1}$ which was not significantly different from non-stretched cells, but significantly different from stretched and non-stretched cells treated with caPKC-ε ($P < 0.05$, n=5, $P < 0.05$, n=5 respectively).

Temporal dynamics of CapZ have been implicated in ischemia-reperfusion models and preconditioning (Yang *et al.,* 2011). The temporal dynamics of CapZβ1 after stretch display a linear reduction in K_{FRAP} rate for approximately 3 hours after the cells have been stretched until reaching the baseline level (Fig. 6B).

Taken together, these results demonstrate that the average CapZβ1 off-rate is increased with mechanical strain or treatment with caPKC-ε. The increased dynamic rate after stretching is abrogated by treatment with dnPKC-ε suggesting a PKCε dependent pathway for mechanotransduction.

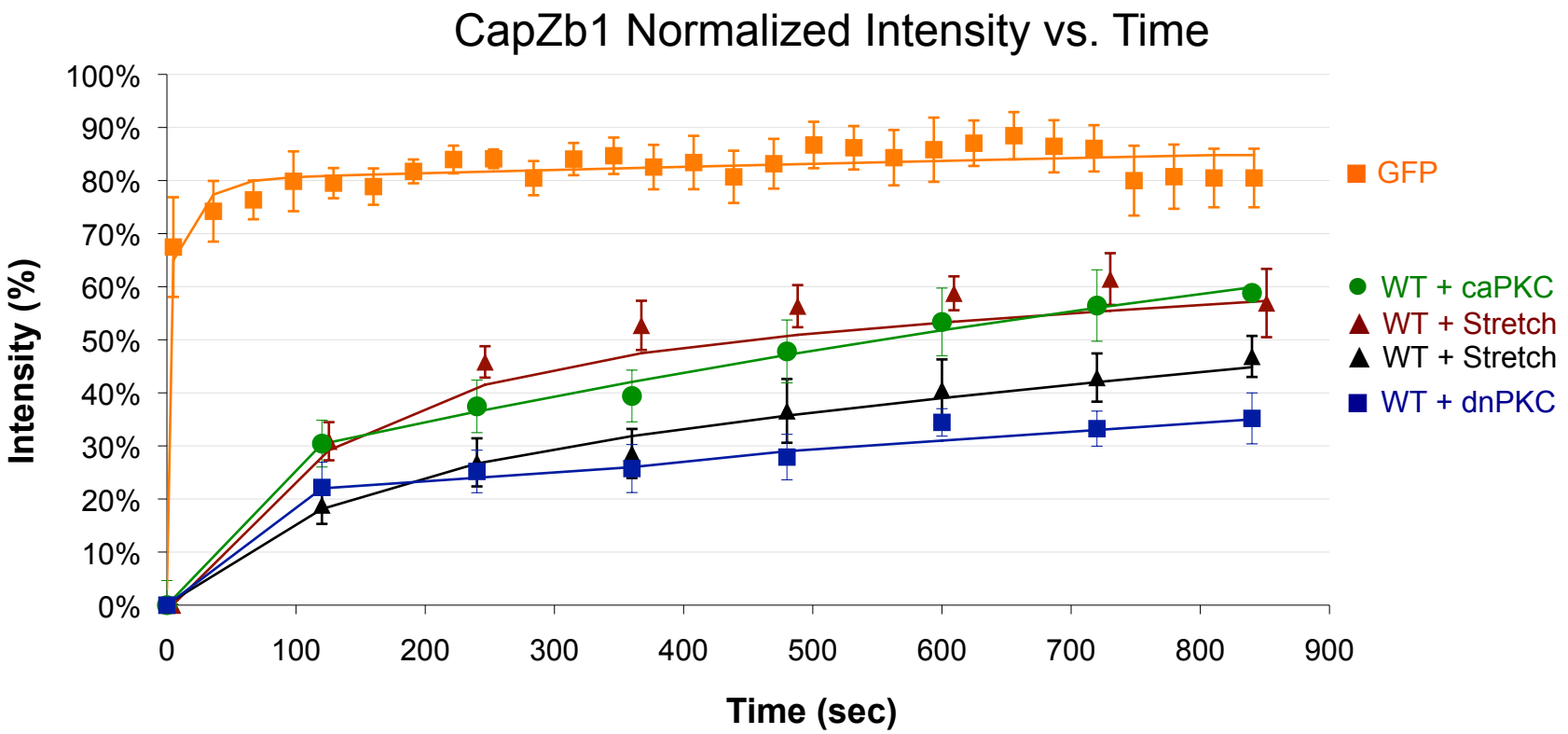

Figure 5. FRAP recovery of GFP-CapZβ1 after mechanical strain and PKC-ε regulation. FRAP analysis was performed on cells expressing WT GFP-CapZβ1 fusion protein. Recovery percentages reported as a percentage of pre-bleach intensity. Cells were cultured for 48 h, infected for 1 h with GFP-CapZβ1 (WT), caPKC-ε (caPKCe), or dnPKC-ε (dnPKCe), and cultured for an additional 24hrs, at which time they were either left untreated, or subjected to 1Hz cyclic, 10% mechanical strain for 1 h (Stretch).

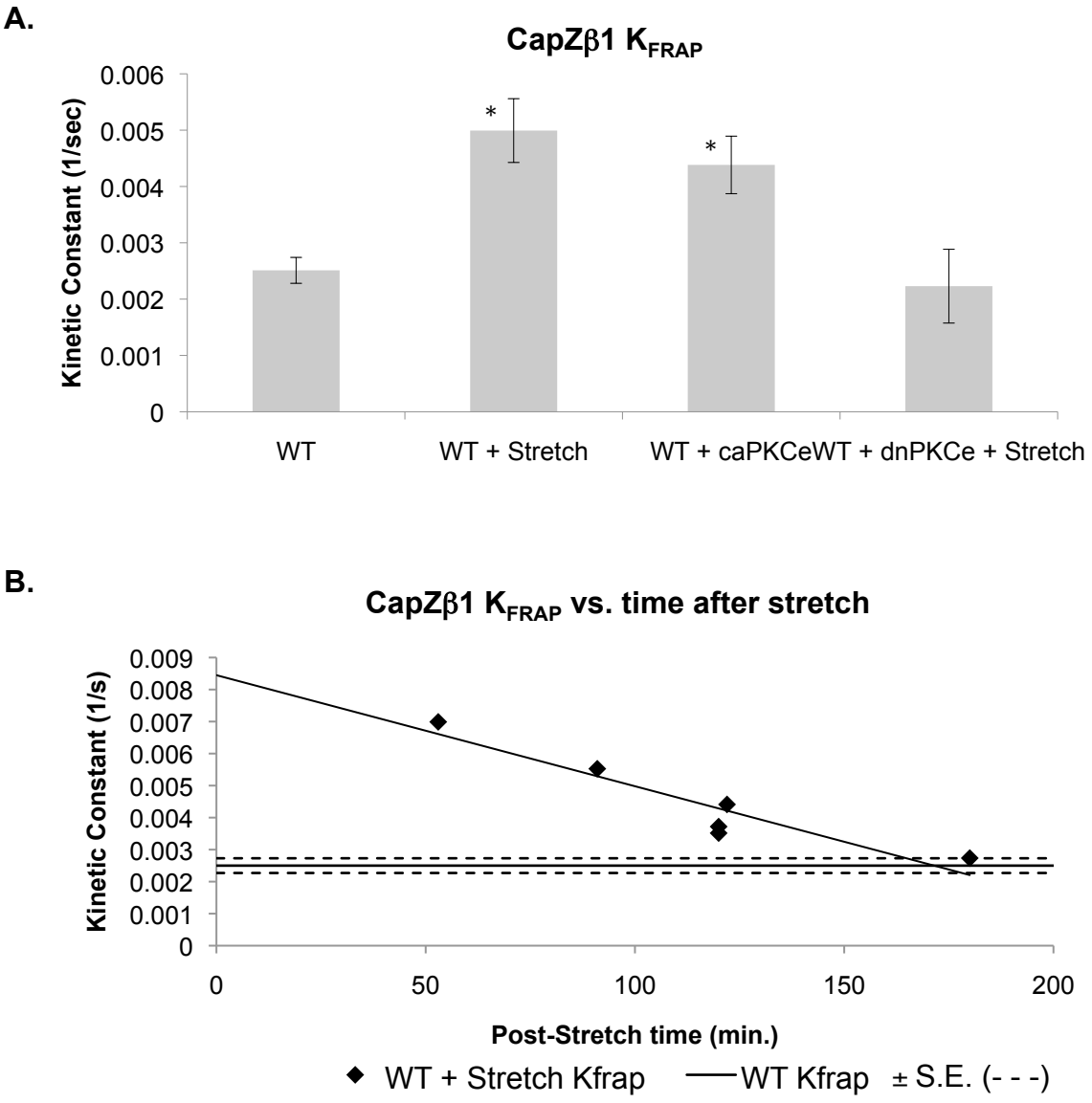

Figure 6. Average and temporal CapZβ1 binding rate response to mechanical strain and PKC-ε regulation. (a) Non-linear regression was used to fit a two binding-state model (*eq.* 3) to individual GFP-CapZβ1 FRAP recovery curves for each condition, and the best-fitting values for the equilibrium and off-rate constants for the fast and slow mobile fraction were combined into an average kinetic constant ($K_{FRAP;}$ *eq. 5*). Data are given as the mean ± SEM (*, $p < 0.05$, n=5). (b) K_{FRAP} values for WT CapZβ1 + stretch were calculated at various time points after treatment of the 1 hour period of mechanical strain (10%, 1Hz, 1 h). Baseline WT CapZβ1 K_{FRAP} given as mean ± SEM (n=5).

Like CapZβ1, CapZβ2 dynamics have also been observed to play a role in cardiac remodeling (Pyle *et al.,* 2002). The FRAP recovery curves obtained for GFP-CapZβ2 are fitted well by the two-binding state equation (3). Qualitatively, the GFP-CapZβ2 FRAP curves are similar in shape to GFP-CapZβ1 recovery curves, however they display a steeper initial slope suggesting a more diffusion coupled process (Fig. 7). Non-stretched cardiomyocyte FRAP response recovery at 15 minutes was 52 ± 6%. Upon treatment of mechanical strain, CapZβ1 recovery at 15 minutes was 72 ± 4%. Non-stretched cells treated with caPKC-ε recovery at 15 minutes was 62 ± 3%. Finally, stretched cells treated with dnPKC-ε recovery at 15 minutes was 51 ± 5%. The free GFP recovery profile characteristically displayed a free-diffusion binding curve as previously mentioned. Recovery at 15 minutes for GFP was 83 ± 5%. The levels of recovery for CapZβ2 do not suggest altered binding affinity of CapZ for actin under each condition.

To measure binding rates quantitatively, every FRAP recovery curve for each condition was fit using the equation (3) and an average kinetic constant, K_{FRAP}, was generated using the equation (5). K_{FRAP} values for each of the conditions do not indicate altered binding dynamics of CapZβ2 after mechanical strain or treatment with caPKC-ε (Fig. 8). Non-stretch control cells had a K_{FRAP} of $7.1 \cdot 10^{-3} \pm 6.9 \cdot 10^{-4} s^{-1}$ which was not significantly different from a K_{FRAP} of $8.9 \cdot 10^{-3} \pm 9.8 \cdot 10^{-4} s^{-1}$ for stretched cells ($P > 0.05$, n=5). Additionally, non-stretched cells treated with caPKC-ε had a K_{FRAP} of $6.5 \cdot 10^{-3} \pm 10.5 \cdot 10^{-4} s^{-1}$ which was not

significantly different from non-stretched cells ($P > 0.05$, n=5). Stretched cells treated with dnPKC-ε had a K_{FRAP} of $6.4 \cdot 10^{-3} \pm 8.9 \cdot 10^{-4} s^{-1}$ was not significantly different from non-stretched cells, stretched cells, or non-stretched cells treated with caPKC-ε ($P > 0.05$, n=5, $P > 0.05$, $P > 0.05$, n=5 respectively).

Taken together, these results indicate that CapZβ2 dynamics are not altered by mechanical strain or PKC-ε.

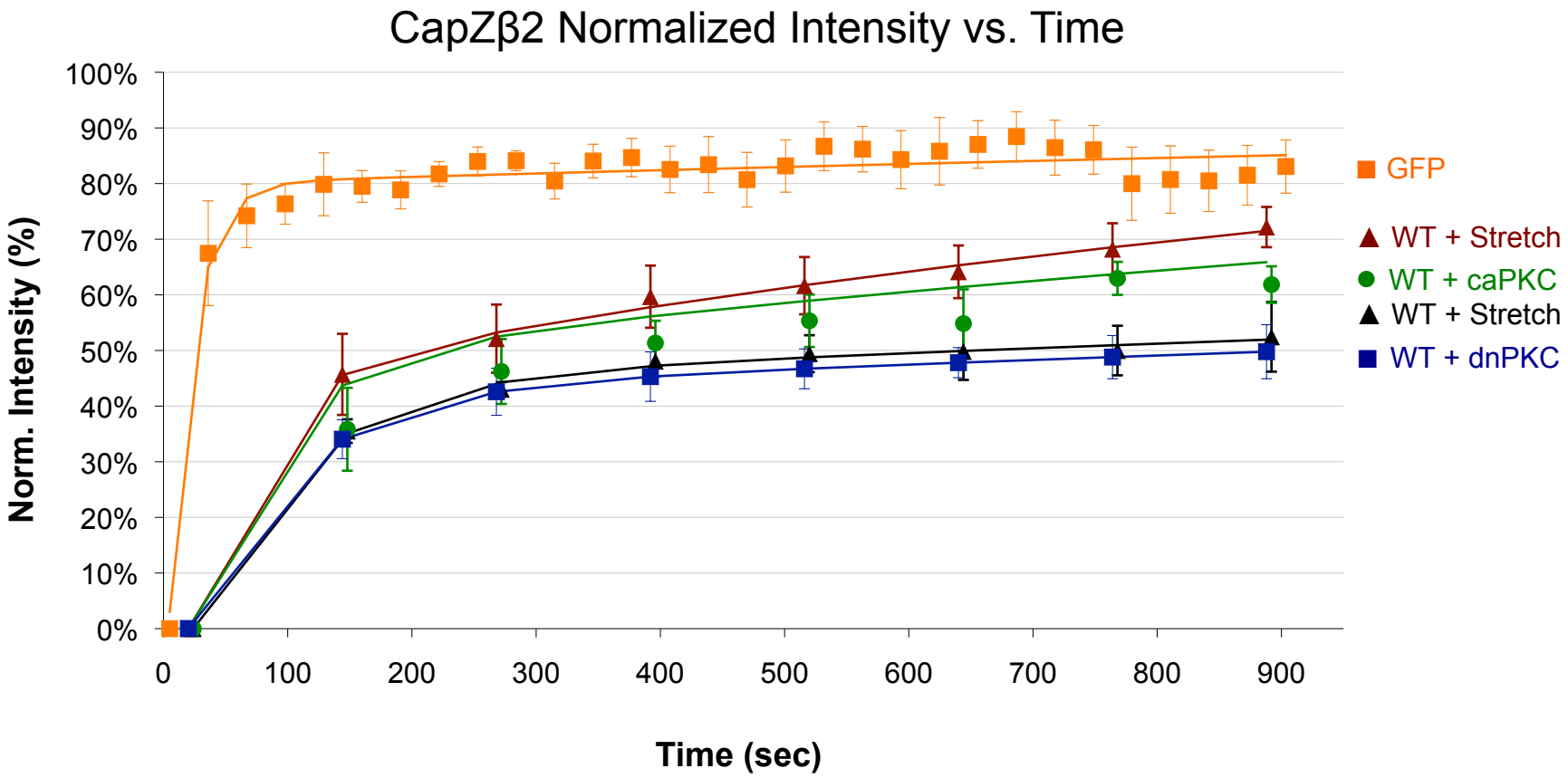

Figure 7. FRAP recovery of GFP-CapZβ2 after mechanical strain and PKC-ε regulation. FRAP analysis was performed on cells expressing WT GFP-CapZβ2 fusion protein. Recovery percentage reported as a percentage of pre-bleach intensity. Cells were cultured for 48 h, infected for 1 h with GFP-CapZβ2 (WT), caPKC-ε (caPKCe), or dnPKC-ε (dnPKCe), and cultured for an additional 24 h, at which time they were either left untreated, or subjected to 1Hz cyclic, 10% mechanical strain for 1 h (stretch).

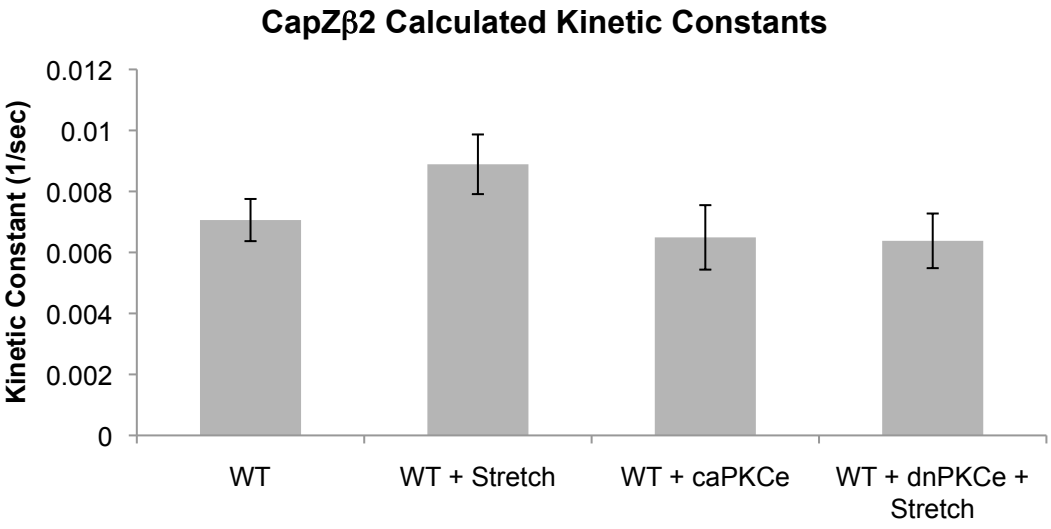

Figure 8. Average CapZβ2 binding rate response to mechanical strain and PKC-ε regulation. Non-linear regression was used to fit a two binding-state model (*eq.* 3) to individual GFP-CapZβ2 FRAP recovery curves for each condition, and the best-fitting values for the equilibrium and off-rate constants for the fast and slow mobile fraction were combined into an average kinetic constant ($K_{FRAP;}$ *eq. 5*). Data are given as the mean ± SEM ($p > 0.05$, n=5).

C. CapZβ1 but not CapZβ2 post-translational profile is altered by mechanical stress and PKC-ε expression

This rapid response of CapZ dynamics to mechanical strain suggests that the alterations in dynamics are not caused by modified gene or protein expression, but rather through post-translational modifications that act on existing proteins or metabolites. Two dimensional gel electrophoresis (2DGE) was used to assess any post-translational modifications of CapZ after stimulation. Staining for CapZβ1 displayed three distinct spots of post-translational modification (Fig. 9A). The three spots were identified at the expected molecular weight of CapZβ1 with isoelectric points of approximately 5.36, 5.24, and 5.13 corresponding to an unphosphorylated form, a singly phosphorylated form, and a doubly phosphorylated form, respectively. Upon treatment of mechanical strain a significant shift in the relative densities between spots was noticed (Fig. 9B). Furthermore, non-stretched cells treated with caPKC-ε also demonstrated a unique alteration in spot density. Stretched cells transfected with dnPKC-ε displayed spot density similar to unstretched controls.

The optical density of all 2DGE spots for each condition was calculated and relative abundance of each spot reported (Fig. 9B). In non-stretched control cells, the abundance of the non-modified, singly modified, and doubly modified form was 37.3 ± 3.2%, 35.1 ± 2.3%, and 27.5 ± 1.3%, respectively. In stretched cells the relative abundance of each form was 31.7 ± 1.7%, 36.6 ± 3.4%, and 31.6 ± 1.8%. In non-stretched cells treated with caPKC-ε the relative abundance of each form was 27.1 ± 0.2%, 43.6 ± 0.4%, and 29.2 ± 0.5%. Finally, in

stretched cells treated with dnPKC-ε the relative abundance of each form was 35.9 ± 2.8%, 32.6 ± 1.1%, and 31.5 ± 1.7%. The only significant difference in abundance of the first form was between non-stretched controls and non-stretched cells treated with caPKC-ε ($P < 0.05$, $n = 3$). Significant difference between the second from was noted between non-stretch cells and cells treated with caPKC-ε ($P < 0.05$, $n = 3$); significant difference was also noted between non-stretch cells treated with caPKC-ε and stretched cells treated with dnPKC-ε ($P < 0.05$, $n = 3$). Finally, the only significant difference noted among the third form was between non-stretch cells and stretched cells ($P < 0.05$, $n = 3$).

The 2DGE results corroborate the CapZβ1 dynamics findings in that only stretched cells, and non-stretched cells treated with caPKC-ε display a significant difference in both post-translational profile and dynamics. These results also suggest that PKC-ε is both necessary and sufficient to alter the post-translational profile of CapZβ1.

To help characterize the differences between CapZβ1 and CapZβ2, the 2DGE study was repeated for CapZβ2. Only one distinct post-translationally modified form of CapZβ2 was observed (Fig. 10A). In non-stretched cells the relative abundance of the non-modified form and singly modified form was 89.4 ± 4.4% and 10.6 ± 4.4% respectively. In stretched the cells the relative abundance was 82 ± 2.2% and 18 ± 2.2%. In non-stretched cells treated with caPKC-ε the relative abundance was 83.9 ± 5.1% and 16.2 ± 5.05%. Finally, in stretched cells treated with dnPKC-ε the relative abundance of each of the forms was 90 ± 2.4% and 10 ± 2.4% (Fig. 10B). There is no significance between any of the data

points. The data for the phosphorylation profile of CapZβ2 also corroborates the CapZβ2 dynamics data in that no significant change in post-translational profile was observed after mechanical stimulation or treatment with PKC-ε.

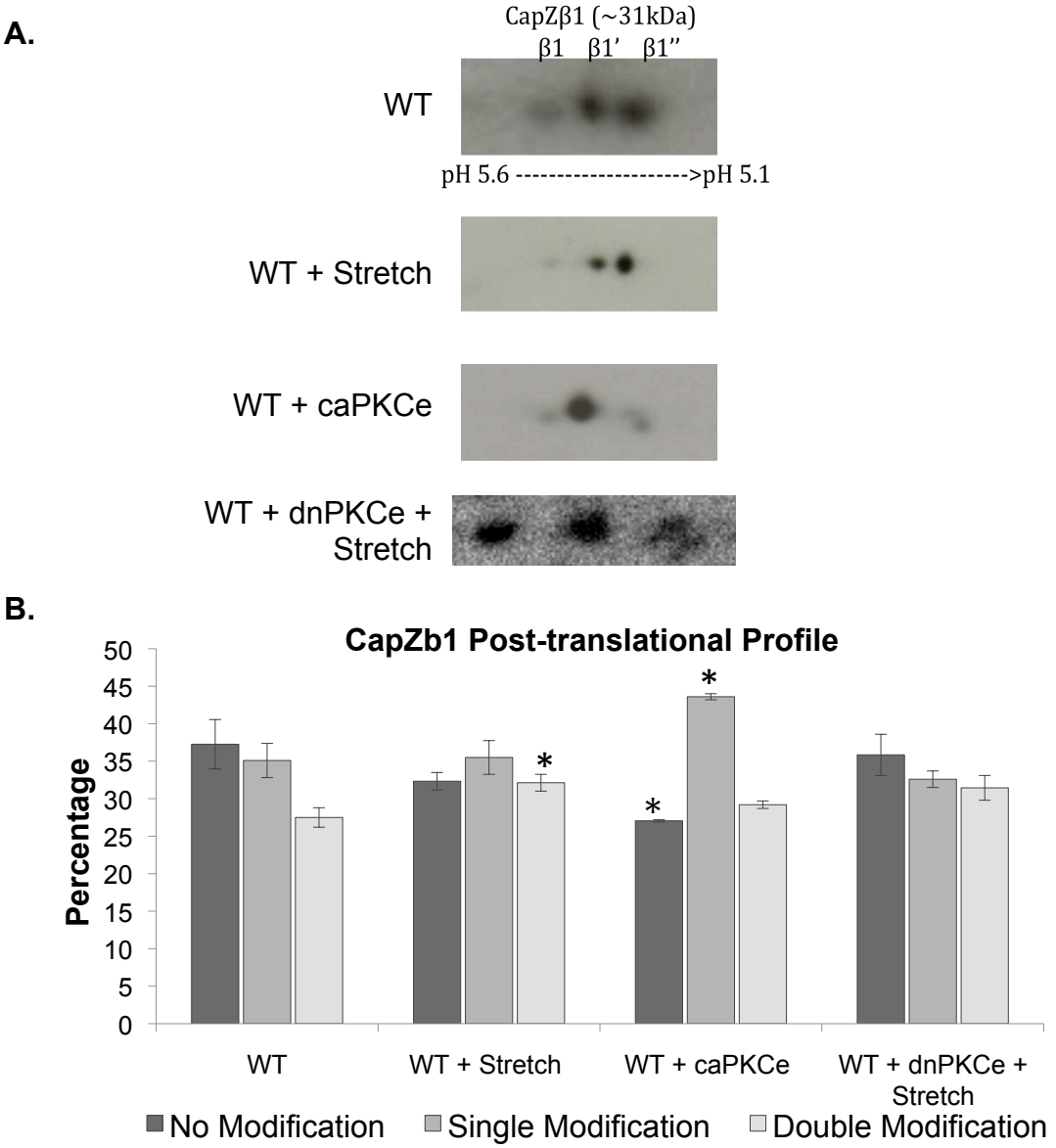

Figure 9. Change in the post-translational profile of endogenous CapZβ1 in response to mechanical strain and PKC-ε regulation. NRVMs were cultured for 48 h, incubated for 1 h with caPKC-ε (caPKCe) or dnPKC-ε (dnPKCe) viral media, or non-viral media, and cultured for an additional 24hrs, at which time they were either left untreated (WT), or subjected to 1Hz cyclic, 10% mechanical strain for 1 h (stretch), immediately lysed and subjected to 2D gel electrophoresis and immunodetection with CapZβ1 IgG. (a) Three distinct spots of post-translational modification for CapZβ1 were detected at ~31kDa and pI of ~5.36, ~5.24, and ~5.13 with varying intensities for each condition. (b) Histogram of relative intensities of each identified spot show mechanical strain and treatment with caPKC-ε alter the post-translational profile of CapZβ1 relative to controls (*, $p < 0.05$, n=3).

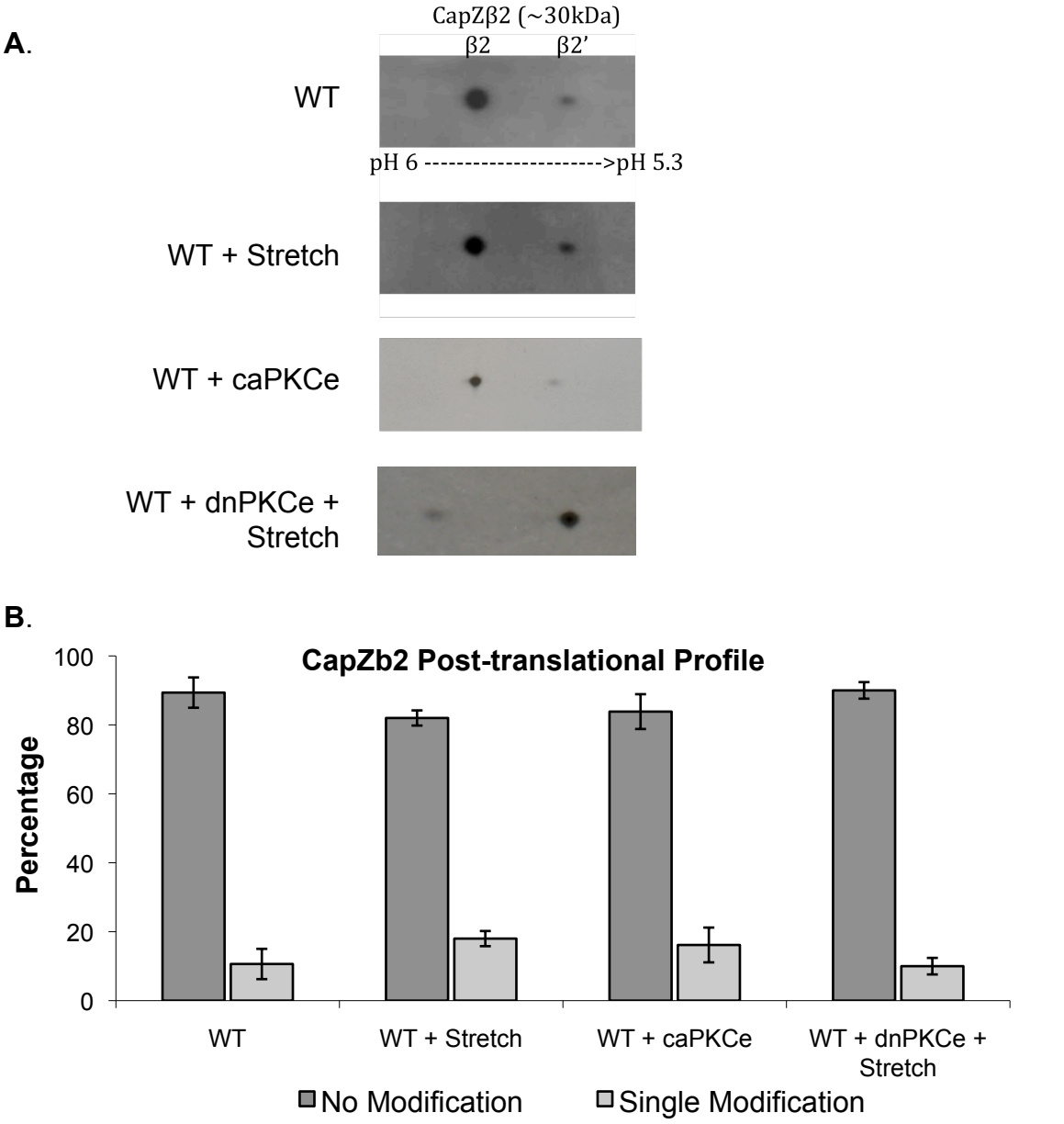

Figure 10. No change in the post-translational profile of endogenous CapZβ2 in response to mechanical strain and PKC-ε regulation. NRVMs were cultured for 48 h, incubated for 1 h with caPKC-ε (caPKCe) or dnPKC-ε (dnPKCe) viral media, or non-viral media, and cultured for an additional 24hrs, at which time they were either left untreated (WT), or subjected to 1Hz cyclic, 10% mechanical strain for 1 h (stretch), immediately lysed and subjected to 2D gel electrophoresis and immunodetection with CapZβ2 IgG. (a) Two distinct spots of post-translational modification for CapZβ2 were detected at ~30kDa and a pI of ~5.69, and ~5.51 with varying intensities for each condition. (b) Histogram of relative intensities of each identified spot show mechanical strain, and treatment with caPKC-ε or dnPKC-ε do not alter the post-translational profile of CapZβ2 relative to controls ($p > 0.05$, n=3).

D. Myofilament protein interactions with CapZβ1

CapZ has been shown to interact with multiple myofilament and signaling proteins that alter its post-translational modification after treatment with mechanical strain or PKC-ε. Co-immunoprecipitation and mass spectrometry was used to identify binding partners of CapZβ1 and specific sites of post-translational modification. Immunoprecipitation with CapZβ1 was performed and the 31kDa band representative of CapZβ1 present in the eluate from the magnetic beads stained strongly with coomassie blue, while very little staining was observed from sample lysate, suggesting high immunoprecipitation efficiency (Fig. 11A). Identification of the proper band for submission to mass spectrometry was confirmed with immunoblotting of CapZβ1 (Fig. 11B). Eight co-immunoprecipitations of CapZβ1 binding proteins from neonatal heart ventricles was performed. A large number of bands stained strongly for coomassie blue suggesting a number of possible interacting proteins of varying size. The analysis of possible interacting proteins is complicated, however, due to the fairly prevalent non-specific binding of proteins to the CapZβ1 antibody. Two bands around ~32kDa and ~30kDa were excised and sent to mass spectrometry services to identify site-specific post-translational modifications of CapZβ1, and identify partnering proteins.

Mass spectrometry was able to determine a specific site of acetylation on CapZβ1, but was unable to detect any other post-translational modifications of CapZβ1. Mass spectrometry identified a total of 43 proteins with a probability greater than 90% (Table I). Due to the amount of non-specific binding of the

CapZβ1 antibody, a great number of proteins were identified. 2DGE western blots stained with CapZβ1 IgG1 were compared against a two-dimensional gel database, and any spots detected by the CapZβ1 antibody that coincided with any mass spectrometry identified proteins were removed from the analysis as non-specific binding partners. The remaining putative binding partners contained ontology related to: cellular processes (6), metabolic processes (2), biological regulation (5), response to stimulus (1), developmental processes (1), localization (1), establishment of localization (1), multicellular organismal process (2), and unknown (2). Three proteins were also identified as having undergone post-translational modifications: oxidation of PDZ-LIM domain proteins 1 and 3, and acetylation of CapZβ (Table I).

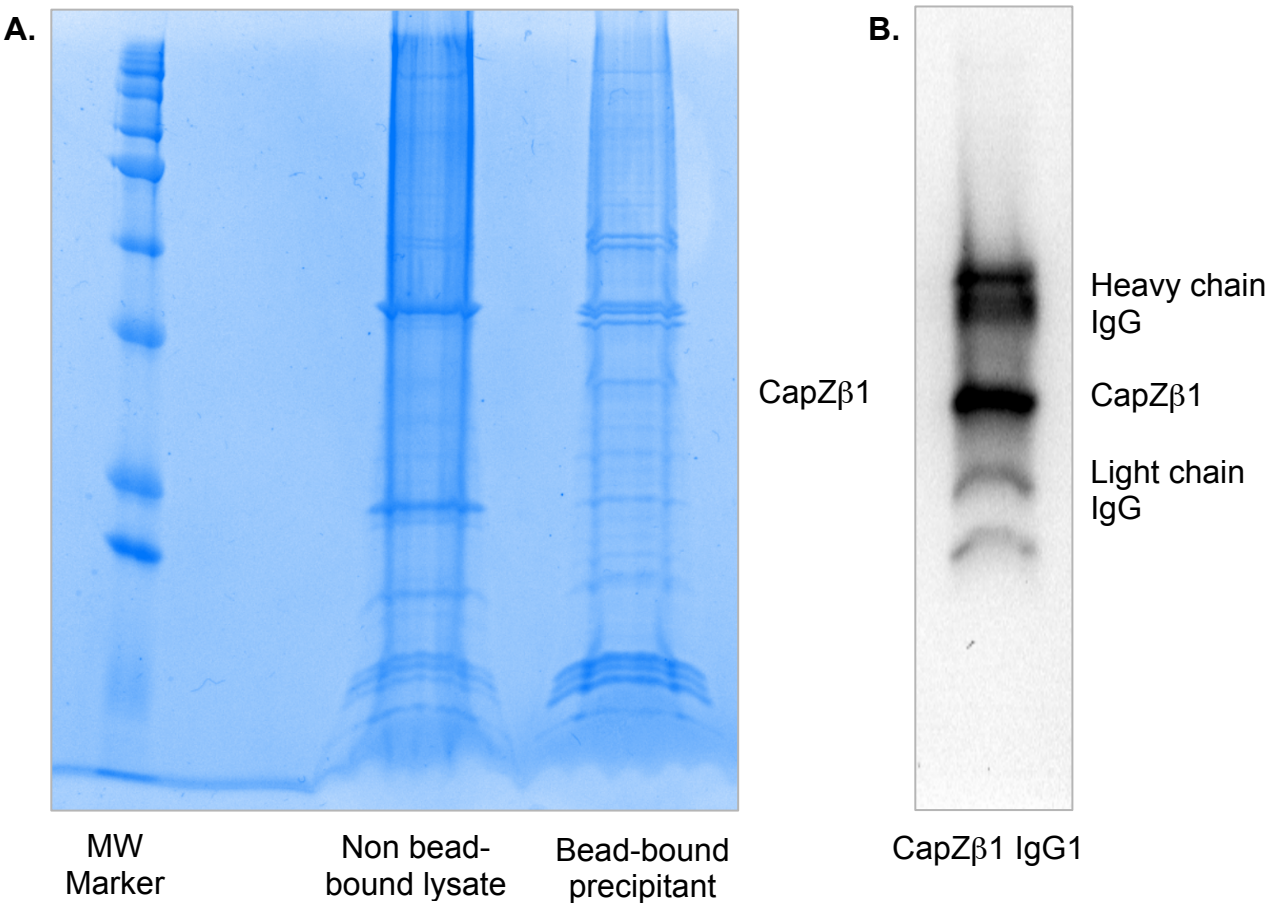

Figure 11. CapZβ1 Immuno- and co-immunoprecipitation from NRVM. 1mg of myofibrillar lysate from neonatal rat ventricles was incubated with 10μg of bead-bound CapZβ1 IgG1. (a) Bead bound protein was precipitated with 8M urea, 2M thiourea, and 4% CHAPS, and run alongside non bead-bound lysate on a 12.5% SDS-acrylamide gel and stained with colloidal coomassie, which detected multiple bands of interacting protein. (b) Western blotting of the bead-bound precipitant gel lane with CapZβ1 IgG confirmed successful immunoprecipitation of CapZβ1 at ~31kDa along with heavy and light chain IgG.

TABLE I
Identification and PTMs of putative CapZβ1 partnering proteins

Oxidation Modified	**Unmodified**
PDZ and LIM domain protein 1	Annexin A2
PDZ and LIM domain protein 3	Cysteine and glycine-rich protein 3 (MLP)
	F-actin-capping protein subunit alpha-1
Acetylation Modified	F-actin-capping protein subunit alpha-2
F-actin-capping protein subunit beta	Four and a half LIM domains protein 2
	Phosphatase PP1-alpha catalytic subunit
	Vimentin

Table I. Identification and PTMs of putative CapZβ1 partnering proteins. 7mg of myofibrillar lysate from neonatal rat ventricles was incubated with 70μg of bead-bound CapZβ1 IgG1. Bead bound interacting proteins were precipitated with 8M urea, 2M thiourea, and 4% CHAPS, and run on a 12.5% SDS-acrylamide gel. Coomassie blue stained bands were excised and digested with trypsin and submitted for tandem mass spectrometry (MS/MS) analysis. MS/MS identified 11 putative CapZβ1 binding partners of which two underwent oxidation modification, one underwent acetylation modification, and seven remained unmodified.

IV. DISCUSSION

This study demonstrates that the alteration of CapZ dynamics and post-translational profile in response to mechanical strain is dependent upon both the subunit isoform of CapZβ and the activity of PKC-ε.

Based upon the quality of fit of the FRAP recovery curve with a two-binding state model, this study demonstrated that CapZ dynamics are governed by multiple affinity states. The two affinity states may arise from conformational changes of CapZ during binding or unbinding reactions supporting a theory of CapZ-actin wobbling proposed by others (Kim *et al.*, 2010). Furthermore, the observation of a rapid response to mechanical strain by the cardiomyocytes suggests that post-translational modification may be an underlying mechanism involved with CapZ-actin binding.

Indeed, many myofilament proteins undergo post-translational modifications in response to strain (Bilsen *et al.,* 1997). This study demonstrates a temporal change in protein dynamics that decline to baseline by three hours after termination of mechanical strain. Furthermore, this study observed two modifications of CapZβ1 that may be regulated uniquely through mechanical or biochemical pathways but achieve the same dynamic result. These findings indicate that CapZ is capable of integrating and responding to several mechanosensing pathways as others have suggested (de Tombe *et al.,* 2000). The dynamics data suggest that CapZ is only able to respond to mechanical strain in a PKC-ε dependent manner, and the proteomic data corroborates this

finding by showing all modifications of CapZ are abrogated when cells are transfected with a dominant negative PKC-ε adenovirus. The mechanism through which strain and PKC-ε are integrated on CapZ remains unknown, however this study offers some mechanistic insight into what may be occurring.

It has been hypothesized that CapZ may bind to actin solely with its β tentacle, allowing it to wobble (Kim *et al.,* 2010). When bound in this wobble state, it may expose binding sites across its surface that can bind CapZ inhibitory or dissociation proteins (Schafer *et al.,* 1996; Takeda *et al.,* 2010). Because the COOH terminal tentacles of both subunits stabilize binding of CapZ to actin, any mechanism that affects the tentacle binding will increase the uncapping rate of CapZ (Takeda *et al.,* 2010).

Previous research demonstrated that the COOH terminal regions of CapZ are amphiphilic and contain both a strongly hydrophobic actin-binding region, and a hydrophilic region capable of binding partnering proteins (Yamashita *et al.,* 2003). Based upon our observations of the dynamic model of CapZ-actin binding, the hydrophobic actin-binding region of CapZ may become accessible when CapZ is bound to actin in its wobble state. The accessible hydrophobic charge present at the Z-disc when CapZ is bound in its wobble state may promote partnering with proteins containing hydrophobic binding regions such as PKC-ε, V-1/myotrophin, PIP2, and others (Bhattacharya *et al.,* 2006).

The observation that CapZ requires active PKC-ε to respond to mechanical strain indicates that PKC-ε regulation plays an important role in actin capping dynamics. It is possible that mechanical strain initiates an IP3/DAG that

generates active PKC-ε through a pathway resembling $G_q\alpha$ activation, which is able to directly modify the secondary structure of CapZ (Hartman *et al.,* 2009), modify CapZ partnering proteins**,** or generate byproducts capable of dissociating CapZ from actin (Schafer *et al.,* 1996) and thereby alter actin capping acitivity.

The structure of PKC-ε, which contains a C-1 region capable of binding hydrophobic surfaces (Zhang *et al.,* 1995), makes it a likely candidate for CapZ binding, although this remains to be studied experimentally. Furthermore, direct binding of active PKC-ε to CapZ and subsequent uncapping may explain the observation of decreased amounts of active PKC-ε in the myofilament fraction of CapZβ1 overexpressed murine hearts observed by Pyle *et al*. (2002). Consistent with the wobble theory of actin binding, mechanical strain is speculated to physically force CapZ into the wobble state, and thus expose PKC-ε binding or target phosphorylation sites. The translocation of PKC-ε to the Z-disc through the binding sites on CapZ, may promote PKC-ε modification of the COOH terminal ends of CapZ, thus greatly reducing its binding affinity to actin and increase uncapping.

The observation that mechanical strain only alters CapZβ1 capping dynamics, but not CapZβ2, provides insight into PKC-ε dependent regulation of capping activity. Although CapZβ1 and CapZβ2 contain sequence and secondary structural similarity, they do contain different COOH terminal sequences that are most likely responsible for their different localization and varying function. This study observed two post-translational modifications of CapZβ1 and only one modification of CapZβ2. In addition, the research also

demonstrated that mechanical strain and treatment with active and inactive PKC-ε only affected CapZβ1. CapZβ2 is the primary non-muscle isoform of CapZβ and may not have evolved to sense and respond to external mechanical stress in a similar manner as CapZβ1.

Although this study is unable to determine all the exact sites, and types, of post-translational modification present on CapZ, the shift in isoelectric points coupled with PKC-ε dependence suggest one possible post-translational modification occurring on CapZ is phosphorylation. In further support of this hypothesis, an isoform specific site of phosphorylation on CapZβ1 has been identified as serine 263 (S263) in the COOH-terminus, making it a likely and accessible site for phosphorylation by PKC-ε (Huttlin *et al.,* 2010; Rigbolt *et al.,* 2011). Previous studies by several groups have shown that modification of the residues of the COOH-terminus of CapZβ1 affect its binding affinity and conformation, and thus may impart a dynamic change on actin capping ability (Hart *et al.,* 1999; Bhattacharya *et al.,* 2006; Kim *et al.,* 2010). This data suggests that PKC-ε may phosphorylate S263, thereby imparting a conformational change on CapZβ1 that may greatly decrease its actin binding ability leading to a functional change in capping protein dynamics. S263 is not present in CapZβ2, and the lack of response of CapZβ2 to mechanical stimulation further supports our hypothesis of a post-translational modification at that site in CapZβ1 and divergent evolutionary adaptation of capping protein isoforms.

In addition to a proposed phosphorylation at S263, an acetylation at S2 was also identified on CapZβ1. The analysis of the observed 2DGE data

suggests the singly modified form would be a phosphorylation of S263, while the doubly modified form would be a phosphorylation of S263 and an acetylation of S2. Because the 2DGE cannot differentiate between sites of phosphorylation we can only hypothesize which site is being modified. In non-stretch cells treated with caPKC-ε we observed a significant increase in the singly phosphorylated form that may be due to phosphorylation of S263 by PKC-ε. This study also observed a significant increase in the doubly phosphorylated form of CapZβ1 after cells were treated with mechanical strain.

Binding of PKC-ε to the cytoskeleton to influence capping activity may also occur through indirect binding of PKC-ε with CapZ partnering proteins. The observed interaction of CapZβ1 with serine/threonine phosphatase 1 alpha (PP1α) may contribute to the temporal dynamics associated with CapZβ1 after mechanical strain through dephosphorylation of the aforementioned modifications. It is possible that mechanical strain causes physical deformation of the Z-disc and uncovers RACKs, which when bound to active PKC-ε, modifies CapZ partnering proteins leading to an increase in the CapZ dissociation rate. This idea has been supported by other groups who have demonstrated that alterations in the Z-disc may change the availability of RACKs (Mochly-Rosen *et al.,* 2000). Whatever the mechanism that causes PKC-ε translocation to the Z-disc and its binding partners, once PKC-ε has localized to the Z-disc it has the ability to interact with many actin cytoskeleton regulatory proteins including CapZ.

Additionally, the difference observed in the post-translational profile of CapZ in response to mechanical strain or caPKC-ε overexpression would suggest that multiple signaling pathways are also operative and may include partnering protein interactions with CapZ.

The results from our co-immunoprecipitation of CapZβ1 confirm a number of interacting myofilament proteins with CapZβ1. Notably, cysteine-lysine rich protein 3, also known as MLP, was found to interact with CapZβ1. MLP deficient mice develop cytoskeletal disruption, dilated cardiomyopathy, and heart failure (Arber *et al.,* 1997; Boateng *et al.,* 2007). Several other LIM proteins were also found to interact with CapZβ1 including four and a half LIM protein 2 (FHL2), which has been shown to modify the hypertrophic response to β-adrenergic stimulation. Similarly to MLP, deficiency of FHL2 in cardiac tissue leads to exaggerated hypertrophy (Kong *et al.,* 2001). Increased MLP sequestration and binding to CapZβ1 in its wobble state would support a positive feedback loop associated with cardiac maladaptation.

Other interactions with PDZ-LIM domain proteins 1 and 3 (CLP-36 and actinin associated LIM protein, respectively) were also observed. Interestingly, ZASP/Cypher, which contains both a PKC-ε binding LIM domain and an α-actinin binding PDZ domain, has been implicated in cytoskeletal remodeling in response to mechanical strain and may affect CapZ dynamics through a similar interaction (Prekeris *et al.,* 1996; Huang *et al.,* 2004). V-1/myotrophin is a small protein that has been identified in hypertrophic rat hearts and human patients with dilated cardiac hypertrophy, and has been shown to inhibit the capping ability of CapZ,

supporting both the wobble hypothesis and increased CapZ partnering protein interaction while CapZ is bound in the wobble state (Sen *et al., 1990*; Sil *et al.,* 1993; Bhattacharya *et al.,* 2006).

Taken together, a speculative mechanism integrates the observation of altered capping dynamics, post-translational modifications, and identification of partnering proteins to explain the response of CapZ to mechanical strain and PKC-ε regulation (Fig. 12). In an unstimulated condition, actin capping and actin polymerization achieve a steady state equilibrium, whereby no remodeling occurs (Fig. 12A). When the cardiomyocytes are mechanically strained, a signaling cascade is initiated that results in the binding of a CapZ partnering protein with CapZ (Fig. 12B). The partnering protein interaction with CapZ induces a post-translational modification on CapZ, causing the CapZα tentacle to dissociate, leaving only the CapZβ attached in its wobble state (Fig. 12C). While in the wobble state, the affinity of active PKC-ε to CapZ greatly increases, leading to a phosphorylation on the COOH terminal end of the β tentacle, which through charge interference causes the β tentacle to dissociate from actin, resulting in complete uncapping (Fig. 12D).

Similarly, when unstrained cells overexpress constitutively active PKC-ε, the increased concentration of PKC-ε overcomes the affinity barrier of PKC-CapZ binding while in the bound state, and leads to a phosphorylation of the β tentacle causing complete uncapping (Fig. 12D). Additionally, in the absence of active PKC-ε, phosphorylation of the β tentacle is unable to occur and capping activity remains unchanged.

The proposed mechanism supports the findings of an increased uncapping rate with stimulation of mechanical strain or consitutively active PKC-ε overexpression. Furthermore, the proposed mechanism explains the observation of a doubly modified form of CapZβ1 after mechanical stimulation, and the observation of a singly modified form of CapZβ1 after consitutively active PKC-ε overexpression which are both dependent upon PKC-ε.

Ultimately, the increase in the actin uncapping rate may be adaptive in that it disrupts the structure of the Z-disc allowing new actin filaments to polymerize or insert, which leads to a global remodeling that decreases the localized load, and therefore strain, at the Z-disc. This feedback loop would support clinical findings of cardiomyopathies in situations of increased load, and constitutively active PKC-ε overexpression in transgenic animals (Takeishi *et al.,* 2000; Strait *et al.,* 2001; Sanger *et al.,* 2008). The present research presents a process by which myocytes subjected to mechanical strain alter their actin capping affinity through a PKC-ε dependent pathway, destabilize the existing cytoskeletal network, and allow the insertion and remodeling of proteins related to heart remodeling.

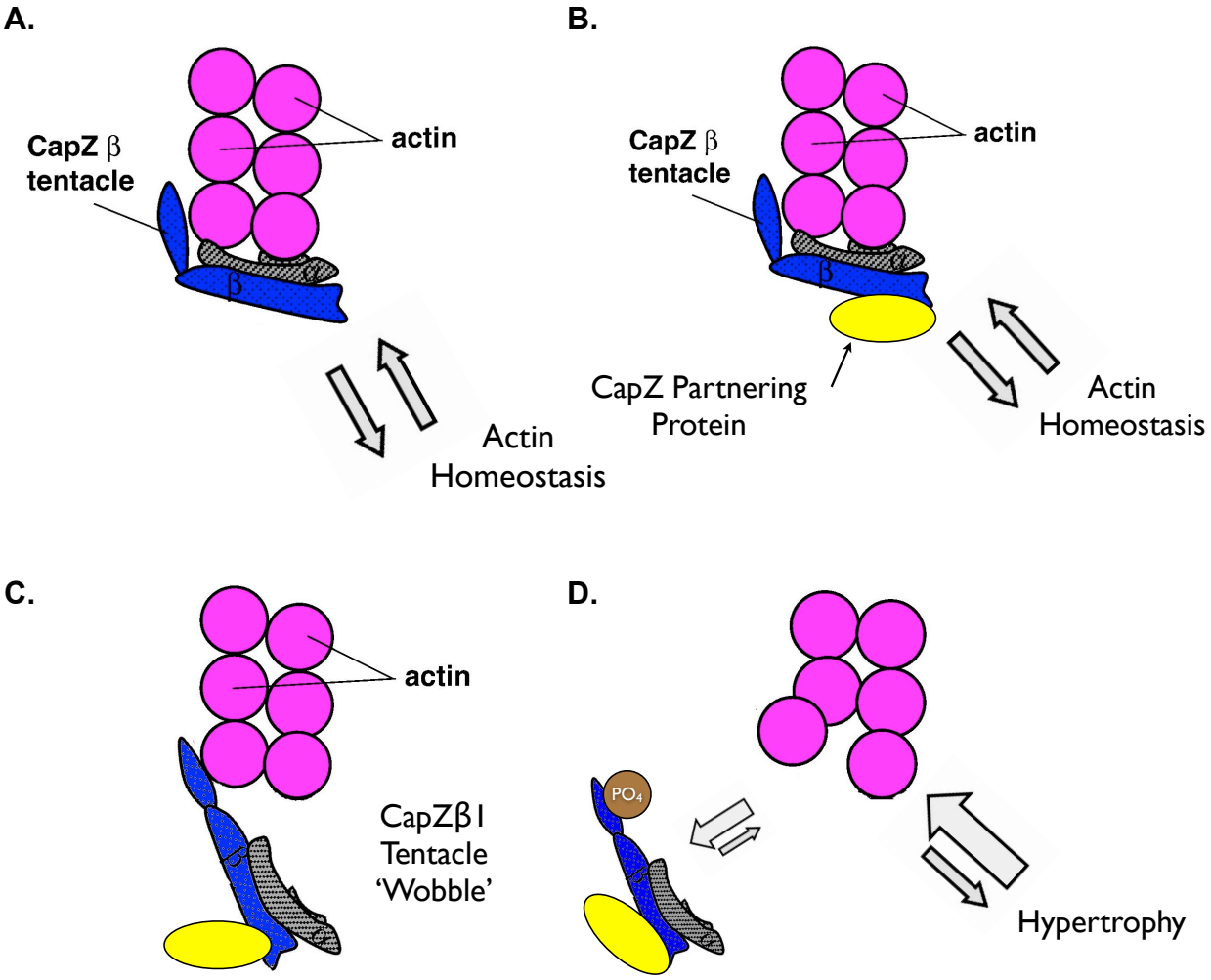

Figure 12. Speculative CapZ-actin dynamic regulation and mechanism for myocyte hypertrophy. (a) In an unstimulated condition, actin capping and actin polymerization achieve a steady state equilibrium, whereby no remodeling occurs. (b) After mechanical stimulation, a signaling cascade is initiated that results in the binding of a CapZ partnering protein with CapZ. (c) The partnering protein interaction with CapZ induces a post-translational modification on CapZ, causing the CapZα tentacle to dissociate, leaving only the CapZβ attached in its wobble state. (d) While in the wobble state, the affinity of active PKC-ε to CapZ greatly increases, leading to a phosphorylation on the COOH terminal end of the β tentacle, which through charge interference causes the β tentacle to dissociate from actin, resulting in uncapping and hypertrophy.

V. CONCLUSIONS

It is clear that the complex environment that CapZ exists within imparts both mechanical and biochemical influence on CapZ dynamics and post-translational profile. This study makes the following conclusions about CapZ and myofilament remodeling:

1. Mechanical strain significantly increases the dissociation rate of CapZβ1 to actin.
2. Constitutively active protein kinase C-ε increases the actin dissociation rate and alters the post-translational profile of CapZβ1 in the absence of external strain.
3. Dominantly negative protein kinase C-ε abrogates any dissociation rate or post-translational influence of mechanical strain on CapZβ1.
4. Many proteins interact with CapZβ1 *in vivo* that may alter the capping dynamics and post-translational profile of CapZ.
5. Mechanical strain does not significantly increase the dissociation rate of CapZβ2 to actin.
6. Neither constitutively active protein kinase C-ε in the absence of external strain, nor dominantly negative protein kinase C-ε in the presence of external strain alters the actin dissociation rate or post-translational profile of CapZβ2.
7. CapZβ1 but not CapZβ2 acts within a PKC-ε dependent mechanotransduction pathway in cardiomyocytes.

VI. FUTURE DIRECTIONS

This study has identified the influence of mechanical strain and protein kinase C-ε on the actin capping dynamics and post-translational profile of CapZ but is limited to rat neonatal ventricular myocytes. The future directions of this study will seek to elucidate the exact mechanism through which the CapZ alterations occur and the applicability of the research to various organisms, and are as follows:

1. Identification of the post-translational modification of CapZ and the site(s) at which it occurs in cultured neonatal rat ventricular myocytes.
2. Identification of the exact PTM and site(s) of modification of CapZ in protein kinase C-ε overexpressing and knockout transgenic mice.
3. Identification of a similar site and mode of modification in failing and non-failing human cardiac tissue.

CITED LITERATURE

Arber, S., Hunter, J.J., Ross, J. Jr., Hongo, M., Sansig, G., Borg, J., Perriard, J., Chien, K., Caroni, P. (1997). MLP-deficient mice exhibit a disruption of cardiac cytoarchitectural organization, dilated cardiomyopathy, and heart failure. *Cell*. 88(3):393-403

Asakura, S. (1961). F-actin adenosine triphosphatase activated under sonic vibration. *Biochim. Biophys. Acta.*, 52: 65-75.

Asakura, S., M. Taniguchi, F. Oosawam. (1963). Mechano-chemical behaviour of F-actin. *J. Mol. Bio.*, 7(1): 55-69.

Barron-Casella, E.A., Torres, M.A., Scherer, S.W., Heng, H.H.Q., Tsui, L.C., Casella, J.F. (1995). Sequence analysis and chromosomal localization of human CapZ. Conserved residues within the actin-binding domain may link CapZ to gelsolin/severin and profiling protein families. *J. Biol. Chem.,* 270:21472-21479.

Bhattacharya, N. Ghosh, S., Sept, D., Cooper, J.A. (2006). Binding of myotrophin/V-1 to actin-capping protein: implications for how capping protein binds to the filament barbed end. *J. Biol. Chem.* 281:31021-31030.

Bilsen, M. (1997). Signal transduction revisted: recent developments in angiotensin II signaling in the cardiovascular system. *Cardio. Research.* 36:310-322

Boateng, S.Y., Senyo, S.E., Qi, L., Russell, B. (2009). Myocyte remodeling in response to hypertrophic stimuli requires nucleocytoplasmic shuttling of muscle LIM protein. *J. Mol. Cell. Cardiol.* 47(4):426-35

Bowling, N., Walsh, R. A., Song, G., Estridge, T., Sandusky, G. E., Fouts, R. L., Vlahos, C. J. (1999). Increased protein kinase C activity and expression of Ca2+-sensitive isoforms in the failing human heart. *Circulation, 99*(3), 384-391.

Cenni, V., Doppler, H., Sonnenburg, E. D., Maraldi, N., Newton, A. C., & Toker, A. (2002). Regulation of novel protein kinase C epsilon by phosphorylation. *Biochem J, 363*(Pt 3), 537-545.

Clark, K. A., McElhinny, A. S., Beckerle, M. C., & Gregorio, C. C. (2002). Striated muscle cytoarchitecture: an intricate web of form and function. *Annu Rev Cell Dev Biol, 18*, 637-706.

Colombo, A., Cahill, P.A., Lally, C. (2008). An analysis of the strain field in biaxial Flexcell membranes for different waveforms and frequencies. *Proc. Inst. Mech Eng.* 222(H):1235-1245

Cooper, G. (2000). Cardiocyte cytoskeleton in hypertrophied myocardium. *Heart Fail Rev, 5*(3), 187-201.

Coussens, L., Parker, P.J., Rhee, L., Yang-Feng, T.L., Chen, E., Waterfield, M.D., Francke, U., Ullrich, A. (1986). Multiple, distinct forms of bovine and human protein kinase C suggest diversity in cellular signaling pathways. *Science*. 233(4766):859-66

Diaz-Flores, E., Siliceo, M., Martinez, A.C., Merida, I. (2003). Membrane translocation of protein kinase Cϕ during T-lympocyte activation requires phospholipase C-γ-generated diacylglycerol. *J. Biol. Chem.* 278:29208-29215

Disatnik, M.H., Buraggi, G., Mochly-Rosen, D. (1994). Localization of protein kinase C isozymes in cardiac myocytes. *Exp Cell Res.* 210:287-297

Dorn, G.W., II, Souroujon, M.C., Liron, T., Chen, C.H., Gray, M.O., Zhou, H.Z., Csukai, M., Wu, G., Lorenz, J.N., Mochly-Rosen, D. (1999). Sustained in vivo cardiac protection by a rationally designed peptide that causes epsilon protein kinase C translocation. *Proc. Natl. Acad. Sci. U.S.A.* 96:12798-12803

dos Remedies, C. G., Chhabra, D., Kekic, M., Dedova, I. V., Tsubakihara, M., Berry, D. A., & Nosworthy, N. J. (2003). Actin binding proteins: regulation of cytoskeletal microfilaments. *Physiol Rev, 83*(2), 433-473.

Eyers, C. E., McNeill, H., Knebel, A., Morrice, N., Arthur, S. J., Cuenda, A., & Cohen, P. (2005). The phosphorylation of CapZ-interacting protein (CapZIP) by stress-activated protein kinases triggers its dissociation from CapZ. *Biochem J, 389*(1), 127-135.

Gorg, A., Postel, W., Gunther, S. (1988). Two-dimensional electrophoresis. The current state of two-dimensional electrophoresis with immobilized pH gradients. *Electrophoresis*. 9:531-546.

Grossman, W., Jones, D., McLaurin, L.P. (1975). Wall Stress and Patterns of Hypertrophy in the human left ventricle. *J. Clin. Invest.* 56(1): 56.

Hart, M. C., Cooper, J. A. (1999). Vertebrate isoforms of actin capping protein beta have distinct functions In vivo. *J Cell Biol, 147*(6), 1287-1298.

Hart, M.C., Y.O. Korshunova, and J.A. Cooper. (1997). Vertebrates have conserved capping protein α isoforms with specific expression patterns. *Cell Motil. Cytoskelet.* 38:120-132.

Hartman, T. J., Martin, J. L., Solaro, R. J., Samarel, A. M., & Russell, B. (2009). CapZ dynamics are altered by endothelin-1 and phenylephrine via PIP2- and PKC-dependent mechanisms. *Am J Physiol Cell Physiol, 296*(5), C1034-1039.

Heidkamp, M. C., Bayer, A. L., Scully, B. T., Eble, D. M., & Samarel, A. M. (2003). Activation of focal adhesion kinase by protein kinase C epsilon in neonatal rat ventricular myocytes. *Am J Physiol Heart Circ Physiol, 285*(4), H1684-1696.

Hishiya, A., Kitazawa, T., Takayama, S. (2010). BAG3 and Hsc70 interact with actin capping protein CapZ to maintain myofibrillar integrity under mechanical stress. *Circ Res, 107*(10), 1220-1231.

House, C., Kemp, B.E. (1987). Protein kinase C contains a pseudosubstrate prototype in its regulatory domain. *Science*. 238:1726-1728

Huang, X., Walker, J. (2004). Myofilament anchoring of protein kinase C-epsilon in cardiac myocytes. *J. Cell Sci.* 117(10):1971-1978.

Huang, X.P., Pi, Y., Lokuta, A.J., Greaser, M.L., Walker, J.W. (1997). Arachidonic acid stimulates protein kinase C-ε redistribution in heart cells. *J. Cell Sci.* 110: 1625-1634

Hug, C., Miller, T. M., Torres, M. A., Casella, J. F., & Cooper, J. A. (1992). Identification and characterization of an actin-binding site of CapZ. *J Cell Biol, 116*(4), 923-931.

Hunter, J. J., & Chien, K. R. (1999). Signaling pathways for cardiac hypertrophy and failure. *N Engl J Med, 341*(17), 1276-1283.

Huttlin EL, *et al.,* (2010). A tissue-specific atlas of mouse protein phosphorylation and expression. *Cell* 143:1174-89.

Inagaki, K., Begley, R., Ikeno, F., & Mochly-Rosen, D. (2005). Cardioprotection by epsilon-protein kinase C activation from ischemia: continuous delivery and antiarrhythmic effect of an epsilon-protein kinase C-activating peptide. *Circulation, 111*(1), 44-50

Inoue, M., Kishimoto, A., Takai, Y., Nishizuka, Y. (1977). Studies on a cyclic nucleotide-independent protein kinase and its proenzyme in mammalian tissues. II. Proenzyme and its activation by calcium-dependent protease from rat brain. *J. Biol. Chem.* 252(21):7610-7616

Isenberg, G., Aebi, U., Pollard, T.D. (1980). A novel actin binding protein from Acanthamoeba which regulates actin filament polymerization and interactions. *Nature* 288, 455-459.

James G, M. (2008). Quantitative FRAP in Analysis of Molecular Binding Dynamics In Vivo. In F. S. Kevin (Ed.), *Methods in Cell Biology* (Vol. Volume 85, pp. 329-351): Academic Press.

Jiang, L., He, L., & Fountoulakis, M. (2004). Comparison of protein precipitation methods for sample preparation prior to proteomic analysis. *J Chromatogr A, 1023*(2), 317-320.

Kim, K., McCully, M.E., Bhattacharya, N., Butler, B., Sept, D., Cooper, J.A. (2007). Structure/Function analysis of the interaction of phosphatidylinositol 4,5-biphosphate with actin-capping protein. *J. Biol. Chem.* 282(8):5871-5879.

Kim, T., Cooper, J. A., & Sept, D. (2010). The interaction of capping protein with the barbed end of the actin filament. *J Mol Biol, 404*(5), 794-802. doi: 10.1016/j.jmb.2010.10.017

Kong, Y., Shelton, J.M., Rothermel, B., Li, X., Richardson, J.A., Bassel-Duby, R., Williams, R.S. (2001). Cardiac-specific LIM protein FHL2 modifies the hypertrophic response to β-adrenergic stimulation. *Circulation.* 103:2731-2738

Kruger, M., Linke, W.A. (2009). Titin-based mechanical signaling in normal and failing myocardium. *J. Mol. Cell. Cardiol.* 46(4):490-498.

Maruyama, K. (1966). Effect of beta-actinin on the particle length of F-actin. *Biochim Biophys Acta, 126*(2), 389-398.

Maruyama, K., & Obinata, T. (1965). Presence of Beta-Actinin in the Soluble Fraction of the Muscle Cells of the Chick Embryo. *J Biochem, 57*, 575-577.

Maruyama, K., Kimura, S., Ishi, T., Kuroda, M., & Ohashi, K. (1977). beta-actinin, a regulatory protein of muscle. Purification, characterization and function. *J Biochem, 81*(1), 215-232.

McNally, J.G. (2008) Quantitative FRAP in analysis of Molecular Binding Dynamics *in vivo*. *Methods Cell Biol.* 85:329-351

Mellor, H., Parker, P.J. (1998) The extended protein kinase C superfamily. *Biochem. J.* 332:281-292

Mochly-Rosen, D. (1995). Localization of protein kinases by anchoring proteins: a theme in signal transduction. *Science*. 268:247-251.

Mochly-Rosen, D., Wu, G., Hahn, H., Osinska, H., Liron, T., Lorenz, J. N., Dorn, G. W., 2nd. (2000). Cardiotrophic effects of protein kinase C epsilon: analysis by in vivo modulation of PKCepsilon translocation. *Circ Res, 86*(11), 1173-1179.

Nakagawa, N., Hoshijimi, M., Oyasu, M., Saito, N., Tanizawa, K., Kuroda, S. (2000). ENH, containing PDZ and LIM domains, heart/skeletal muscle-specific protein, associates with cytoskeletal proteins through the PDZ domain. *Biochem. Biophys. Res. Commun.* 272:505-512

Narita, A., Takeda, S., Yamashita, A., Maeda, Y. (2006). Structural basis of actin filament capping at the barbed-end: a cryo-electron microscopy study. *EMBO J.* 25(23):5626-5633

Newton, A. C. (1995). Protein kinase C: structure, function, and regulation. *J Biol Chem, 270*(48), 28495-28498.

Nishizuka, Y. (1986). Studies and perspectives of protein kinase C. *Science*. 233(4761):305-312

Olson TM, Doan TP, Kishimoto NY, Whitby FG, Ackerman MJ, Fananapazir L. 2000. In- herited and de novo mutations in the cardiac actin gene cause hypertrophic cardiomyopathy. *J. Mol. Cell. Cardiol.* 32:1687–94

Olson TM, Michels VV, Thibodeau SN, Tai YS, Keating MT. 1998. Actin mutations in dilated cardiomyopathy, a heritable form of heart failure. *Science* 280:750–52

Phair, R. D., Gorski, S. A., & Misteli, T. (2003). Measurement of Dynamic Protein Binding to Chromatin In Vivo, Using Photobleaching Microscopy. In C. D. Allis & W. Carl (Eds.), *Methods in Enzymology* (Vol. Volume 375, pp. 393-414): Academic Press.

Ping, P., Zhang, J., Qiu, Y., Tang, X. L., Manchikalapudi, S., Cao, X., & Bolli, R. (1997). Ischemic preconditioning induces selective translocation of protein kinase C isoforms epsilon and eta in the heart of conscious rabbits without subcellular redistribution of total protein kinase C activity. *Circ. Res.* 81(3), 404-14.

Prekeris, R., Mayhew, M.W., Cooper, J.B., Terrian, D.M. (1996) Identification and localization of an actin-binding motif that is unique to the epsilon isoform of protein kinase C and participates in the regulation of synaptic function. *J. Cell. Biol.* 132:77-90

Pyle, W. G., Solaro, R. J. (2004). At the crossroads of myocardial signaling: the role of Z-discs in intracellular signaling and cardiac function. *Circ Res, 94*(3), 296-305

Pyle, W. G., Hart, M.C., Cooper, J. A., Sumandea, M. P., de Tombee, P. P., Solaro, R. J. (2002). Actin capping protein: an essential element in protein kinase signaling to the myofilaments. *Circ. Res.* 90:1299-1306. *Circ Res, 81*(3), 404-414.

Rigbolt, K.T., Prokhorova, T.A., Akimov, V., Henningsen, J., Johansen, P.T., Kratchmarova, I., Kasem, M., Mann, M., Olsen, J.V., Blagoev, B. (2011). System-wide temporal characterization of the proteome and phosphoproteome of human embryonic stem cell differentiation. Sci. Signal. 4(164):rs3

Robia, S.L., Ghanta, J. Robu, V.G., Walker, J.W. (2001). Localization and kinetics of protein kinase C-ε anchoring in cardiac myocytes. *Biophys J.* 80:2140-2151

Rosse, C., Linch, M., Kermorgant, S., Cameron, A. J., Boeckeler, K., & Parker, P. J. (2010). PKC and the control of localized signal dynamics. *Nat Rev Mol Cell Biol, 11*(2), 103-112.

Samarel, A. M. (2005). Costameres, focal adhesions, and cardiomyocyte mechanotransduction. *Am J Physiol Heart Circ Physiol, 289*(6), H2291-2301.

Sanger, J.M., Sanger, J.W. (2008). The dynamic Z bands of striated skeletal muscle cells. *Sci. Signal* 1:pe37.

Schafer, D. A., Korshunova, Y. O., Schroer, T. A., & Cooper, J. A. (1994). Differential localization and sequence analysis of capping protein beta-subunit isoforms of vertebrates. *J Cell Biol, 127*(2), 453-465.

Schafer, D.A., Waddle, J.A. Localization of CapZ during myfibrillogenesis in cultured chicken muscle. (1993). *Cytoskeleton*. 25(4):317-335

Sen, S., Kundu, G., Mekhail, N., Castel, J., Misono, K., and Healy, B. (1990). Myotrophin: purification of a novel peptide from spontaneously hypertensive rat heart that influences myocardial growth. *J. Biol. Chem.* 27**,** 16635–16643

Sil, P., Misono, K., Sen, S. (1993). Myotrophin in human cardiomyopathic heart. *Circ Res.* 1:98-108

Solaro, R. J. (2010). Sarcomere control mechanisms and the dynamics of the cardiac cycle. *J Biomed Biotechnol, 2010*, 105648. doi: 10.1155/2010/105648

Spitaler, M., & Cantrell, D. A. (2004). Protein kinase C and beyond. *Nat Immunol, 5*(8), 785-790. doi: 10.1038/ni1097

Sprague, B. L., & McNally, J. G. (2005). FRAP analysis of binding: proper and fitting. *Trends Cell Biol, 15*(2), 84-91. doi: 10.1016/j.tcb.2004.12.001

Sprague, B. L., Pego, R. L., Stavreva, D. A., & McNally, J. G. (2004). Analysis of binding reactions by fluorescence recovery after photobleaching. *Biophys J, 86*(6), 3473-3495. doi: 10.1529/biophysj.103.026765

Stout, A. L., Wang, J., Sanger, J. M., & Sanger, J. W. (2008). Tracking changes in Z-band organization during myofibrillogenesis with FRET imaging. *Cell Motil Cytoskeleton, 65*(5), 353-367

Strait, J. B., 3rd, Martin, J. L., Bayer, A., Mestril, R., Eble, D. M., & Samarel, A. M. (2001). Role of protein kinase C-epsilon in hypertrophy of cultured neonatal rat ventricular myocytes. *Am J Physiol Heart Circ Physiol, 280*(2), H756-766.

Takeda, S., Minakata, S., Koike, R., Kawahata, I., Narita, A., Kitazawa, M., Nitanai, Y. (2010). Two distinct mechanisms for actin capping protein regulation--steric and allosteric inhibition. *PLoS Biol, 8*(7), e1000416.

Takeishi, Y., Ping, P., Bolli, R., Kirkpatrick, D. L., Hoit, B. D., & Walsh, R. A. (2000). Transgenic overexpression of constitutively active protein kinase C epsilon causes concentric cardiac hypertrophy. *Circ Res, 86*(12), 1218-1223.

Taylor, S.S., Radzio-Andzelm, E. (1994). Three protein kinase structures define a common motif. *Structure*. 2:345-355

von Bulow, M., H.R. Rackwitz, R. Zimbelmann, W.W. Franke. (1997). CP β-3, a novel isoform of an actin-binding protein, is a component of the cytoskeletal calyx of the mammalian sperm head. *Exp. Cell Res.* 233:216-224

Warren, C. M., Geenen, D. L., Helseth, D. L., Jr., Xu, H., & Solaro, R. J. (2010). Sub-proteomic fractionation, iTRAQ, and OFFGEL-LC-MS/MS approaches to cardiac proteomics. *J Proteomics, 73*(8), 1551-1561.

Wear, M. A., Yamashita, A., Kim, K., Maeda, Y., & Cooper, J. A. (2003). How capping protein binds the barbed end of the actin filament. *Curr Biol, 13*(17), 1531-1537.

Wear, M.A., Cooper, J.A. (2004) Capping protein binding to S100B: Implications for the tentacle model for capping the actin filament barbed end. *J. Biol. Chem.* 279:14382-14390

Weber, A., Pennise, C. R., Babcock, G. G., & Fowler, V. M. (1994). Tropomodulin caps the pointed ends of actin filaments. *J Cell Biol, 127*(6): 1627-1635.

Yamashita, A., Maeda, K., & Maeda, Y. (2003). Crystal structure of CapZ: structural basis for actin filament barbed end capping. *EMBO J, 22*(7), 1529-1538. doi: 10.1093/emboj/cdg167

Yang, F. H., Pyle, W. G. (2011). Reduced cardiac CapZ protein protects hearts against acute ischemia-reperfusion injury and enhances preconditioning. *J. Mol. Cell Cardiol*. doi: 10.1016/j.yjmcc.2011.11.013

Zhang, G., Kazanietz, M.G., Blumberg, P.M., Hurley, J.H. (1995). Crystal structure of the cys2 activator-binding domain of protein kinase C delta in complex with phorbol ester. *Cell.* 81:917-924.

Zhou, Q., Ruiz-Lozano, P., Martone, M.E., Chen, J. (1999). Cypher, a striated muscle-restricted PDZ and LIM domain-containing protein, binds to alpha-actinin-2 and protein kinase C. *J. Biol. Chem.* 274:19807-19813

APPENDIX

UIC UNIVERSITY OF ILLINOIS AT CHICAGO

Office of Animal Care and Institutional
Biosafety Committee (OACIB) (M/C 672)
Office of the Vice Chancellor for Research
206 Administrative Office Building
1737 West Polk Street
Chicago, Illinois 60612

11/16/2011

Brenda Russell
Physiology & Biophysics
M/C 901

Dear Dr. Russell:

The protocol indicated below was reviewed in accordance with the Animal Care Policies and Procedures of the University of Illinois at Chicago and **renewed on 11/16/2011.**

Title of Application: **Isolation of Heart Cells From Neonatal Rats**
ACC NO: **10-189**
Original Protocol Approval: **1/6/2011 (3 year approval with annual continuation required).**
Current Approval Period: **11/16/2011 to 11/16/2012**

Funding: ***Portions of this protocol are supported by the funding sources indicated in the table below.***
Number of funding sources: 1

Funding Agency	**Grant Title**			**Portion of Grant Matched**
NIH	*Integrated Mechanisms Of Cardiac Maladaptation (Tied to Form G 10-098)*			*Matched*
Grant Number	**Current Status**	**UIC PAF NO.**	**Performance Site**	**Grant PI**
PO1 HL062426 (years 11-15)	*Funded*	*2009-06478*	*UIC*	*Grant PI- R. John Solaro/Project 2 PI- Brenda Russell*

This institution has Animal Welfare Assurance Number A3460.01 on file with the Office of Laboratory Animal Welfare, NIH. **This letter may only be provided as proof of IACUC approval for those specific funding sources listed above in which all portions of the grant are matched to this ACC protocol.**

Thank you for complying with the Animal Care Policies and Procedures of the UIC.

Sincerely,

Richard D. Minshall

Richard D. Minshall, PhD
Chair, Animal Care Committee

RDM/*kg*
cc: BRL, ACC File

VITA

Education

UNIVERSITY OF ILLINOIS AT CHICAGO COLLEGE OF MEDICINE Department of Physiology and Biophysics	M.S.	08/10-05/12
RENSSELAER POLYTECHNIC INSTITUTE COLLEGE OF ENGINEERING Department of Biomedical Engineering Biomechanics Concentration	B.S.	08/04-05/08

Abstracts / Publications

Swanson, E., Warren, C., Solaro, R.J., Samarel, A.M., Russell B. “Cyclic mechanical strain alters CapZb1 but not CapZb2 dynamics and phosphorylation via PKCe-dependent mechanisms for cell hypertrophy.”

Teaching Experience

Teaching Assistant – Introduction to Biology (2008, 09)

Professional Experience

2009-2010 – Research Specialist in Physiology and Biophysics
Department of Physiology and Biophysics
University of Illinois at Chicago
Brenda Russell, Ph.D. – Professor of Physiology and Biophysics

- Performed primary cultures and advanced proteomic techniques
- Mastered advanced microscopy techniques involving quantitative live cell imaging

Summer 2007 - Research & Design Engineer
DFine Inc., San Jose, CA
Eric Buehlmann, M.S.

- Contributed towards development of a medical device for kyphoplasty
- Performed cadaver studies using operating room procedures, C-Arm fluoroscope, and bone cement
- Involved with FDA compliance, UL standards, CE certification, 510(k) certification, and ASTM testing standards

Societies / Awards

- Alpha Epsilon Delta
- Alpha Eta Mu Beta
- Phalanx Honor Society
- Order of Omega
- Biomedical Engineering Society
- Graduate Poster Prize – UIC Center for Cardiovascular Research
- *Cum Laude* Graduate
- AP Scholar